MATERIALS CHEMISTRY FRONTIERS

REVIEW

View Article Online
View Journal | View Issue

Cite this: *Mater. Chem. Front.*, 2021, **5**, 129

Design of functionally cooperating systems and application towards self-propulsive mini-generators

Mengjiao Cheng, †*[a] Lina Zhang †[b] and Feng Shi *[a]

The research field of smart materials exhibits a systematic trend with multiple cooperative materials for achieving complex tasks. Recently, the research on 'functionally cooperating systems' has arised as a solution to address this systematic demand, namely, the integration of two or more smart materials into one device to make them function cooperatively for designated missions. In particular, research on the self-propulsion of miniature smart devices *via* functionally cooperating systems has demonstrated advanced uses such as mini-generators, biomimicking devices, macroscopic supramolecular assembly, and directed transportation. Among them, mini-generators that convert the kinetic energy from motion to electrical energy hold promise for improving the energy diversity with interdisciplinary efforts and achievements owing to the integrated and cooperative characteristics of smart devices. To review the recent progress of functionally cooperating systems, herein, we introduce this research field with emphasis on the demonstration of self-propulsion, summarize the underlying principles for integrating multiple smart materials with typical examples, demonstrate the application of self-propulsive mini-generators based on horizontal/vertical and other reciprocating motions, uses of self-propulsion in macroscopic supramolecular assembly and directed transportation. We believe that an insight into functionally cooperating systems may motivate innovative strategies for the systematic integration of smart materials.

Received 27th July 2020,
Accepted 11th September 2020

DOI: 10.1039/d0qm00548g

rsc.li/frontiers-materials

[a] *State Key Laboratory of Chemical Resource Engineering & Beijing Laboratory of Biomedical Materials & Beijing Advanced Innovation Center for Soft Matter Science and Engineering, Beijing University of Chemical Technology, Beisanhuan East Road 15, Beijing, 100029, China. E-mail: chengmj@mail.buct.edu.cn, shi@mail.buct.edu.cn*

[b] *School of Pharmaceutical Sciences, Hebei Medical University, Zhongshan East Road 361, Shijiazhuang, 050017, China*

† These authors contributed equally.

1. Introduction

For decades, smart materials have facilitated the development of material science from a passive status to an active stage. The research interest has moved from simple preparation to stimuli-responsive design, which covers abundant smart examples with response to pH, light, temperature, magnet, electric field, *etc.*[1–6]

Mengjiao Cheng

Dr Mengjiao Cheng is an associate professor at the Beijing University of Chemical Technology. She received her BSc (2010) and PhD (2015) from the Beijing University of Chemical Technology in Prof. Feng Shi's group, and joined Prof. Lifeng Chi's group for post-doctoral research (2015–2016) in Muenster University (Germany). Her ongoing research is on precise macroscopic supramolecular assembly.

Lina Zhang

Dr Lina Zhang was born in Hebei, China, in 1991. She received her PhD (2019) from the Beijing University of Chemical Technology. Afterwards, she took a position at Hebei Medical University as a lecturer. Her research is focused on smart devices, micro–nano motors, and their applications, such as energy conversion and drug delivery.

Nowadays, the research field of smart materials has a systematic and cooperative demand for realizing complex tasks or functions.[7–12] For example, multifunctional actuators are designed with multiple materials responsive to several stimuli (heat, pH, light) to induce deformations, on–off switching, and fluorescent display.[13] Biomimicking the colour shifting behaviours of chameleons requires coordination of several smart materials, for *e.g.*, vapochromic and vapomechanical responses for colour and shape changes actively.[14] Therefore, similar to computers with highly integrated characteristics, the research field of smart materials has a trend towards the integration of diverse smart materials with a high level of cooperation.

The recently developed 'functionally cooperating systems'[15–24] describe the aforementioned new characteristics of smart materials: systems with the integration of two or more smart materials in one device, which could function in a sequential manner to complete designated missions (Scheme 1).[16] Notably, the description of 'cooperating' is different from the existing concept of 'cooperativity'[25–28] in molecular interactions with multiple receptors/ligands (*e.g.*, oxygen binds to hemoglobin). Here, 'cooperating' refers to the cooperation between different materials with specific functions in a designated manner, which resembles the cooperation of many components in integrated electronics following certain programs. This idea of 'functionally cooperating systems' is significant especially for self-propulsions or robotic systems at the miniature length scale from micrometer to centimetre. Nanoscale or meter-sized systems already have powerful toolkits to integrate multiple components; micromanipulation could be realized by optical tweezer, probes of scanning tunneling microscope, magnetic field, *etc.* The manufacture of bulky systems relies on the robust mechanical engineering or techniques to build more complex robotic systems. However, miniaturized systems are too large for micromanipulation techniques and too small for traditional mechanical manufacture.[29] Therefore, strategies to integrate smart materials into miniaturized systems following the idea of 'functionally cooperating systems' is lacking, and imply both challenges and opportunities for innovations in materials science and chemistry.

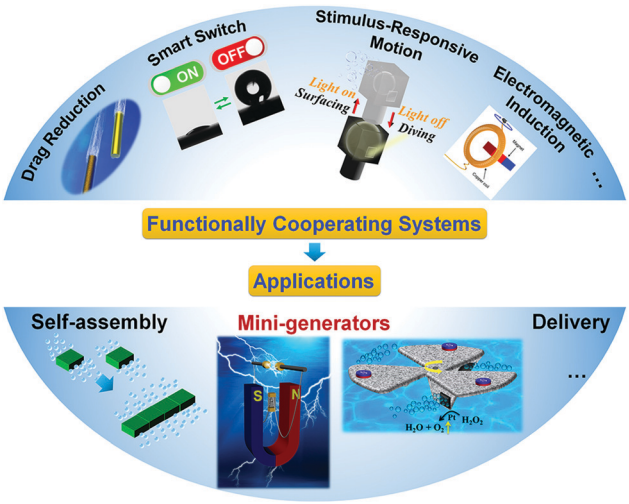

Scheme 1 Schematic illustration of 'functionally cooperating systems', which integrate multiple functions (*e.g.*, drag reduction,[41] smart switching,[42] responsive motion,[23] and electromagnetic induction[43]) into one system, and applications (*e.g.*, self-assembly[32] and mini-generators[19,44]) of such integrative systems. Adapted with permission from ref. 41, Copyright 2007 Wiley; ref. 42, Copyright 2014 Wiley; ref. 23, Copyright 2018 Wiley; ref. 43, Copyright 2015 Springer Nature; ref. 32, Copyright 2014 Wiley; ref. 19, Copyright 2014 Wiley; ref. 44, Copyright 2016 American Chemical Society.

To date, the progress achieved in reports related to 'functionally cooperating systems' has been mainly focused on the self-propulsion of miniaturized devices. These devices have been demonstrated for application in advanced research fields or practical uses including mini-generators,[18,19,24,30] biomimicking devices,[22,31] macroscopic supramolecular assembly,[32–34] and directed transportation.[17,35] The underlying principle of these demonstrations is to convert other forms of energy into kinetic energy, such as chemical energy released from chemical reactions,[16] mechanical energy from periodic motions of organ activities,[36] even environmental energy stored in light,[23] pressure difference,[22] heat,[37–39] *etc.* Depending on the end use of self-propulsive devices, the manner of motion differs ranging from reciprocating motions for electricity generation,[19] one-shot motions mimicking emergency escape of beetles from predators,[31,40] to random motions for insight into self-assembly behaviours.[32,34] Taken together, the design of miniaturized devices aimed at self-propulsion generally includes: (1) the preparation of smart devices with integrated functions of drag reduction, smart switching, stimulus-responsive motion, electromagnetic induction, *etc.*; (2) motion control over horizontal or vertical movements, on/off status, moving speed and turning directions; (3) efforts to improve the energy conversion rates by minimizing the dissipated energy; (4) exploitation of applicable scenarios of such self-propulsion.

Among the applications of self-propulsive devices based on functionally cooperating systems, mini-generator is an attractive topic with rapid development and much progress[18,19,23,24,30,43,45]

Feng Shi

Prof. Feng Shi received his BSc (2001) and MSc (2004) from Jilin University, and PhD (2007) from Tsinghua University under the supervision of Prof. Xi Zhang, during which he was involved in cooperative research with Prof. Harald Fuchs and Prof. Lifeng Chi (Muenster University, Germany) in 2002, and with Prof. Itamar Willner (Hebrew University of Jerusalem, Israel) in 2005. After post-doctoral research at Max Planck Institute for Polymer Research with Prof. Wolfgang Knoll, he joined the Beijing University of Chemical Technology as a full professor (2008). His research interest is macroscopic supramolecular assembly.

in increasing the diversity of power supply. Despite this, traditional power supply (*e.g.*, batteries) dominates in daily life; most micro-electronics (*e.g.*, micro-sensors and implanted devices) do not necessarily consume high-grade energy for power supply because they only need a low power level at μW or mW.[46] Therefore, mini-generators hold promise as alternative matching strategies for powering low energy-cost electronics with additional advantages of being sustainable and cost-effective for the benefit of energy economy and environment. Generally, a mini-generator is referred to as a centimetre-sized or below device/apparatus that could convert other forms of energy into electrical energy. Currently, there are mainly two categories of mini-generators. One is known as triboelectric nanogenerator (TENG) that was first demonstrated by Wang's group;[47–50] the other is self-propulsive mini-generators based on functionally cooperating systems.[18,19] TENG mainly converts mechanical energy in contact-separation motions into electrical energy *via* the combination of triboelectric effect and electrostatic induction, and has been covered comprehensively by abundant reviews.[51–56] Self-propulsive mini-generators are designed following the classical Faraday's law of electromagnetic induction by converting the kinetic energy in reciprocating motions into electrical energy, which relies on the integration and cooperation of multiple smart materials. Even though self-propulsive mini-generators have been an active research field, their progress is yet to be summarized.

In this review, we have introduced the research field of functionally cooperating systems with diverse applications in advanced fields of mini-generators, self-assembly, delivery, *etc.* (Scheme 1). Firstly, the idea of 'functionally cooperating systems' has been described with examples of self-propulsive smart devices. Secondly, the underlying design principle of self-propulsive smart devices is summarized according to different energy input and integration methods. Thirdly, self-propulsive mini-generators are demonstrated based on horizontal/vertical and other reciprocating motions as well as hybridization with TENG. Finally, other applications of self-propulsion-based functionally cooperating systems are shown in macroscopic supramolecular assembly and directed transportation based on functionally cooperating systems. The characteristics of functionally cooperating systems correspond well with the development trend of smart materials with systematic and integrative features to satisfy the demand of increasing intelligence of artificial material systems. We envision the future advancement of this research field owing to its interdisciplinary connections and its emphasis on programmability/cooperativity between components.

2. Functionally cooperating systems

Functionally cooperating systems refer to systems with the integration of two or more smart materials in one device, which could function in a sequential manner to complete designated missions.[16] The emergence of functionally cooperating systems satisfies the demand of increasing the programmability and 'intelligence' of smart materials, which requires the integration and cooperation of multiple components similar to artificial robotic systems and natural creatures to complete complex tasks[57] or biological activities. Recent research has revealed the reasons for the fast colour changes of chameleons:[58] they have two superimposed groups of iridophores responsible for adjusting the guanine nanocrystal spacing in a lattice and reflecting light in the near-infrared range. The effective combination of different iridophores with different functions allows for active and fast response to display environment changes *via* the fine tuning of neural or hormonal mechanisms. In artificial mechanical engineering, such as intelligent robotic systems, similar feedback loops of input–output with programs is requisite for completing designated missions. As for material science, smart materials represent a progress from a passive stage with more focus on the structures at an active stage with emphasis on stimulus-responsive behaviours. However, simply relying on one smart material could hardly realize complex functions such as the colour change of chameleons or robotic movements.

Functionally cooperating systems have provided a feasible solution for integrated and cooperative functions, especially for the design of self-propulsive smart devices of miniaturized sizes.[59] Taking a self-propulsive mini-motor in the vertical direction as an example,[16] the smart device consists of a smart surface with a pH-responsive wettability property, a wrapped platinum responsive to hydrogen peroxide, and a cubic moving part with flexible density fluctuation (Fig. 1a). The cycled diving-surfacing movement could be realized *via* cooperation between the components (Fig. 1b): when the smart surface is 'turned off' with a superhydrophobic property under acidic conditions (pH = 1), the device floats on the solution surface; upon changing the conditions to alkaline (pH = 13), the smart surface exhibits wettability conversion from superhydrophobicity to superhydrophilicity due to the responsive property of the mixed thiols with methyl and carboxylic acid groups; meanwhile, the wetted device allows for the infiltration of the solution into the interior, accompanied by an increase in the total density, leading to the diving process; after adding HCl and H_2O_2 solutions sequentially, the surface changes back to hydrophobic and oxygen bubbles are generated along with the decomposition reaction of H_2O_2 catalysed by platinum, resulting in propelling solutions out of the device to reduce the total density and to provide buoyancy for re-surfacing. The above design represents a typical functionally cooperating system for realizing self-propulsive diving-surfacing motions owing to the integrated multiple responsive materials and the coordination with each other.

3. Design principles of functionally cooperating systems

The design of functionally cooperating systems for self-propulsive purposes includes three key parts: the propulsion system, the motion control system, and the functional system. Unlike nanoscale

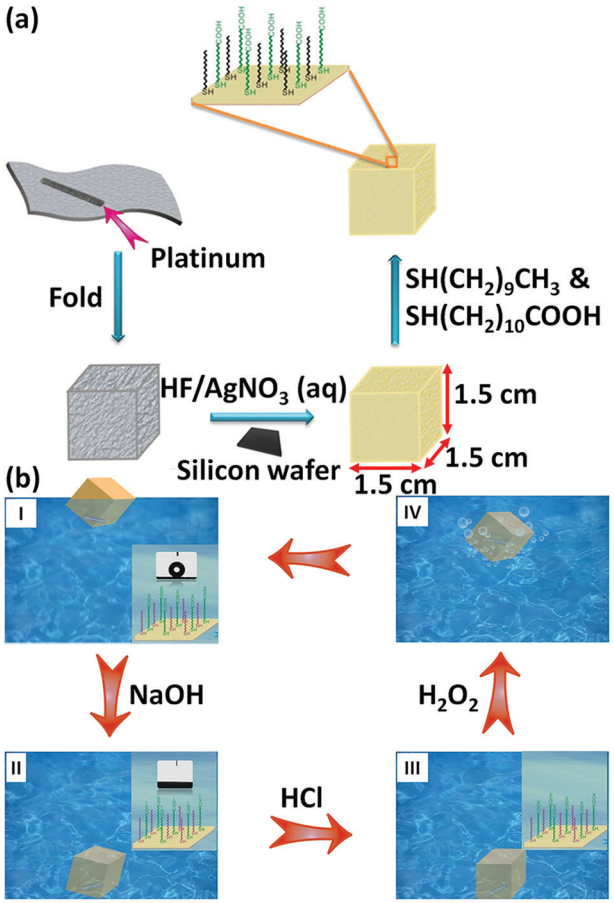

Fig. 1 (a) Integration of functionally cooperative components for the fabrication of a self-propulsive device; (b) the cycled diving-surfacing movement realized *via* cooperation between the components. Adapted with permission from ref. 16. Copyright 2010 Wiley.

manipulation and meter-sized mechanical manufacture, the preparation of self-propulsive smart devices requires alternative methods to load the above main parts due to the paradox at this length scale: the manufacturing scale is too large for microfabrication and too small for conventional machining.[29] In particular, the fabrication of self-propulsive devices is challenging because of the difficulty in handle driving forces and motion control: molecular thermal motion becomes too weak to propel objects with a size from tens of micrometres to centimetres; meanwhile, traditional manufacturing is confronted by challenges as surface forces are dominant over inertial forces, mechanical joints are less efficient, manufacturing precision are hard to reach, and electric machinery power are difficult to install. Therefore, creative strategies for converting other diverse energy forms into kinetic energy have been developed.

For the key unit of propulsion systems, the design principle for horizontal motions is loading driving forces based on chemical energy[16] or surface tension gradient[31] and simultaneously inducing drag reducing coatings.[60–64] For millimetre-sized objects, energy from chemically reactive systems such as H_2O_2 (catalysed by Pt[65] or Pd[18]), Mg–HCl,[19] and $CaCO_3$–HCl[21] could be used for forward/upward motions by jetting gas bubbles in these chemical reactions. Alternately, long-range fluidic forces in Marangoni effects with surface tension gradient, induced by concentration or temperature difference at the interface, have been demonstrated to be effective in propelling macroscopic devices of millimetre or centimetre dimensions.[31,33,66–68] At the same time, the integration of drag reduction functions is favourable for reducing the energy cost and for improving the moving velocity of devices moving on/in fluids. For the propulsion system of vertical motions, the design principle for self-propulsion is the fine and reversible tuning of the device density.[19,69] By triggering chemical reactions that release gas bubbles, extra buoyancy is provided to decrease the device density for a surfacing process; after bubble release at the air/water interface, the device density is tuned back to result in a diving process. Besides, for a certain amount of bubbles trapped within the device, controlled pressure change could also induce a volume change of the gas and density fluctuation.[22,23,36]

For the motion control system, smart surfaces with responsive properties are integrated to act as a switch. For example, in cases of devices for vertical motions, smart surfaces with a pH-responsive switch for surface wettability[16,19] could block or trigger the infiltration of solutions into the device, leading to total density. Integration of other switch in response to temperature change,[17] photo stimulus,[66] *etc.*, which largely enriches the strategies for motion control such as directed turning around[66] and on/off/on motions.[70] Moreover, two or more switches could be integrated into the same device to realize complex motion behaviours such as reciprocating movement in the horizontal direction by loading two switches at the opposite ends of the device.[20]

The design of functional systems based on self-propulsion of smart devices is flexible according to the energy source and the intended use. For example, a self-propulsive device used for active 'search' and collection of spilt oil is normally designed with an open container of superhydrophobic properties, which functions cooperatively with self-propulsion to absorb spilt oil.[35,71] A device designated as a self-propulsive mini-generator normally combines with a magnetic field and an output circuit. In particular, mini-generators designed for power supply of low-energy-cost electronics such as a gas flowmeter are further integrated to a practical industrial line.[72] Mini-generators that harvest low-grade energy from the environment normally require connection with a energy source such as an apparatus to focus sunlight,[23] an apparatus to generate gas bubbles in real industry line, and a connection to the blood cycle to collect the energy stored in the blood pressure.[36]

Taken together, instead of relying on molecular thermal motions or electrical machinery systems, the design of miniaturized self-propulsive devices based on functionally cooperating systems shows a feature with considerations of multiple factors including input energy, driving forces, drag reduction, and applicable scenarios. The general key units of propulsion, motion control, and functional systems are highly integrated with cooperative characteristics and related to the purpose of end use.

4. Self-propulsive mini-generators based on functionally cooperating systems

Self-propulsive mini-generators, which convert the kinetic energy of reciprocating motions into electrical energy based on Faraday's law, represent an attractive and promising application of functionally cooperating systems. The underlying mechanism of self-propulsive mini-generators is the relative motions between the magnets and the conductors, which results in a periodic change in the magnetic flux and induced current in the circuit. Accordingly, a self-propulsive mini-generator consists of a self-propulsive system, a magnetic field (permanent magnets), and an output circuit for electricity storage and end use. All components are cooperative with each other to realize a steady power supply. Similar to the design principle of self-propulsion of functionally cooperating systems, self-propulsive mini-generators mainly have two forms of motions, including horizontal rotation and vertical diving/surfacing movement. Other motions such as torsional rotation or bending movements have been applied for mini-generators as well. The main driving forces include surface tension gradient *via* Marangoni effect, bubble propulsion based on chemical reactions, and responsive deformation triggered by pressure difference, light, and moisture.

4.1 Self-propulsive mini-generators *via* horizontal rotation

Self-propulsion in the horizontal direction has been applied for electricity generation by applying driving forces such as Marangoni flows and bubble release. Marangoni effect, which was first observed as a phenomenon of 'tears of wine' in 1855 by James Thomson and studied by Carlo Marangoni, refers to mass transfer along the interface between two fluids as a result of the gradient of the surface tension. By learning from insects propelling themselves on the surface of water after releasing surfactants,[40] researchers have applied Marangoni effect in the self-propulsion of miniaturized devices.[73,74] Moreover, a stimulus-responsive switch is integrated with Marangoni propulsive systems to yield control over the motion status and moving direction.[31] Further integration with magnetic fields leads to mini-generators harvesting free-energy change in the Marangoni effect.[24,30,75]

An early work on self-propulsive mini-generators based on the Marangoni effect was demonstrated by Osada and co-workers.[15,76] They placed an amphiphilic polymer gel, *e.g.*, poly(stearyl acrylate), which was swollen in ethanol or tetrahydrofuran, onto the surface of water. The synergetic effects caused by osmotic pressure difference and hydrostatic pressure after the contraction of the surface gel layer ejected ethanol out of the gel and generated a propulsive force in the opposite direction, leading to a random motion (Fig. 2a). To regulate the motion trajectory, they made a gel rotor with a central stator as the pivot and two spouting holes at opposite sides of the gel ends for ethanol release; other parts of the gel were wrapped with an aluminium foil. Moreover, two permanent magnets were attached to the ends of the rotor and a solenoid coil was placed above the motion area, which was connected to an output circuit. With the above integration of multiple functional components, the rotor rotates clockwise and induces a maximum electromotive force of 15 mV and an output power of 0.2 μW (Fig. 2b), which could light a photodiode after amplification. This principle has demonstrated a feasible strategy to combine the Marangoni effect with Faraday's law. Recently, Zhang *et al.* reported diverse motions of miniature robots driven by loading concentrated droplets consisting of polyvinylidene fluoride/dimethyl formamide,[30] which produces the Marangoni effect on water; similarly, the kinetic energy of the droplet could be converted to electrical energy by regular rotations.

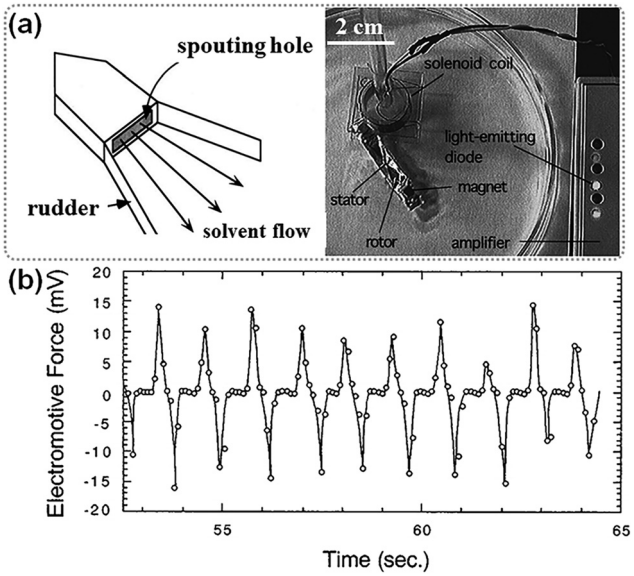

Fig. 2 (a) Schematic illustration of the gel rotor and photographs of the self-propulsive mini-generator; (b) electromotive force generated by the self-propulsive mini-generator. Adapted with permission from ref. 15. Copyright 1998 AIP Publishing.

Further efforts on self-propulsive mini-generators based on the Marangoni effect have been made for improving the moving velocity and energy conversion rate, and prolonging the lifetime. For example, Matsui *et al.* have proposed a self-propulsive mechanism by integrating a metal–organic framework (MOF) and diphenylalanine peptide (DPA), which could be stored/released from the MOF and generates a strong surface tension gradient around the MOF due to its accumulation after release (Fig. 3a).[77,78] The motion could be triggered by mixing sodium ethylenediaminetetraacetate (Na-EDTA) to partially break the MOF structures for the release of DPA and its re-assembly to form a surface tension gradient. The generated driving force was sufficient to propel macro-sized plastic boats on water (Fig. 3b); therefore, they have designed a peptide–MOF mini-generator loaded with a permanent magnet and harvested electrical energy by rotation below the coil (Fig. 3c).[78] The self-propulsive mini-generator is efficient with a maximum induced potential of 0.4 V and an output of 0.1 μW per rotation (Fig. 3d). The velocity of normalized volume, the kinetic energy

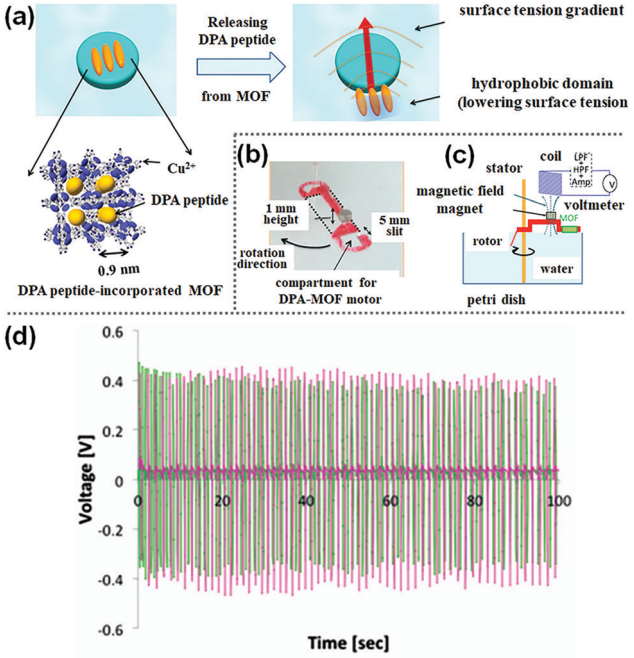

Fig. 3 (a) Illustration of the DPA–MOF motor and its moving mechanism; (b) a macro-sized plastic boat driven by the DPA–MOF motor; (c) schematic illustration of the self-propulsive mini-generator; (d) induced voltage generated from the DPA–MOF mini-generator. Adapted with permission from ref. 78. Copyright 2015 Wiley.

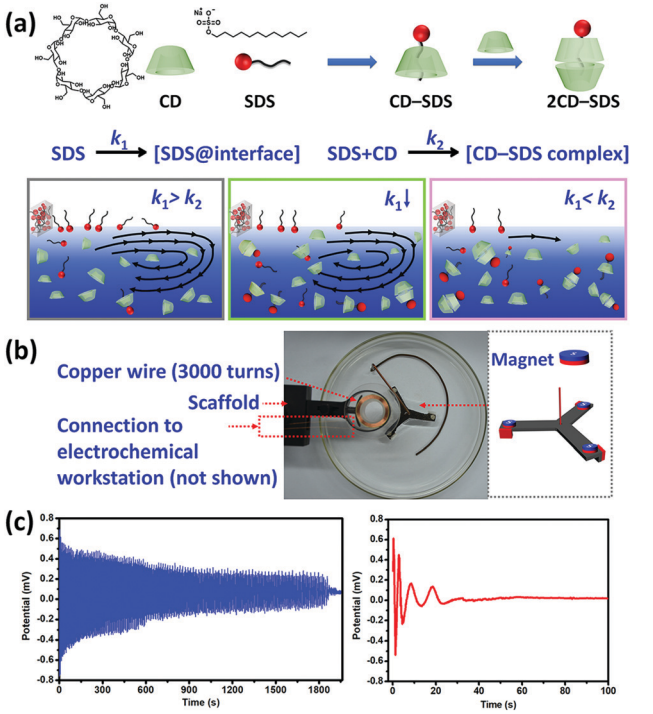

Fig. 4 (a) The competitive equilibria between the interfacial adsorption of the surfactant (SDS) and dissolution after complexation with CD; (b) apparatus of the self-propulsive mini-generator based on the prolonged Marangoni effect; (c) comparison of induced voltage with (left) and without (right) the supramolecular strategy. Adapted with permission from ref. 75. Copyright 2019 Chinese Chemical Society.

per unit mass of fuel, and the electromagnetic force were all improved compared to the gel motor systems. This may be due to the fine storage and release mechanism with the MOF structures and the fine tailoring of the peptide self-assembly at the molecular level.

However, amphiphilic surfactants with both a hydrophilic end and a hydrophobic end have the problem of gradual aggregation and saturation of the air/water interface, especially in a limited water area.[79] To address this problem and meanwhile to tailor the motion behaviour at the molecular level, we have proposed a supramolecular strategy by inducing competitive equilibria between interfacial adsorption and dissolution (Fig. 4a).[75] We encapsulated a typical surfactant molecule of sodium dodecyl sulphate (SDS) in hydrogels as the fuel of Marangoni motions of a rotor, and meanwhile, added a host molecule of β-cyclodextrin (CD) in water, which could form a water-soluble complex with SDS. The equilibria compete between SDS adsorption, which tends to saturate the interface, and SDS dissolution into water by its complexation with CD, which tends to clear SDS at the interface. As a result, a steady surface tension gradient could be maintained to ensure prolonged Marangoni rotation by about 40-fold. By further integrating with a superhydrophobic rotor for reducing fluidic drag and magnets, electricity generation was remarkably prolonged from less than 20 s in the case without using this strategy to 1800 s.

Other methods to avoid the problem of surfactant saturation at the interface mainly use specific volatile chemicals such as camphor[79–81] and alcohol[82–84] or soluble species.[85] These chemicals have high surface activity, which results in strong Marangoni flow and meanwhile could be removed from the interface *via* evaporation to maintain a steady surface tension gradient. For example, Bormashenko and co-workers fabricated a mini-generator consisting of a polymer rotor loaded with 'camphor engines' and magnets (Fig. 5a).[24] The evaporation of camphor, followed by its adsorption at the vapor/water interface, could form Marangoni flows to propel the rotor. The rotation is long-lasting for 10–20 h. Besides Marangoni effects, the driving forces provided by chemical reactions that generate bubbles could also be used for the design of a mini-generator based on horizontal rotation. For example, we have fabricated a mini-generator based on a functionally cooperative system (Fig. 5b)[44] consisting of (1) a fan-like rotor with three blades with drag reducing performance due to superhydrophobic coatings, (2) three 'platinum engines' made of rough platinum structures for efficiently catalysing the decomposition of hydrogen peroxide, and (3) three magnets on each blade to produce a varied magnetic flux in rotation. This mini-generator could last for 26 000 s with one filling of hydrogen peroxide.

4.2 Self-propulsive mini-generators *via* vertical rotation

Mini-generators based on vertical motions follow another design principle of fine fluctuation of density. Normally, self-propulsion exhibits a reciprocating diving/surfacing manner due to the reversible density change of the total device. At a

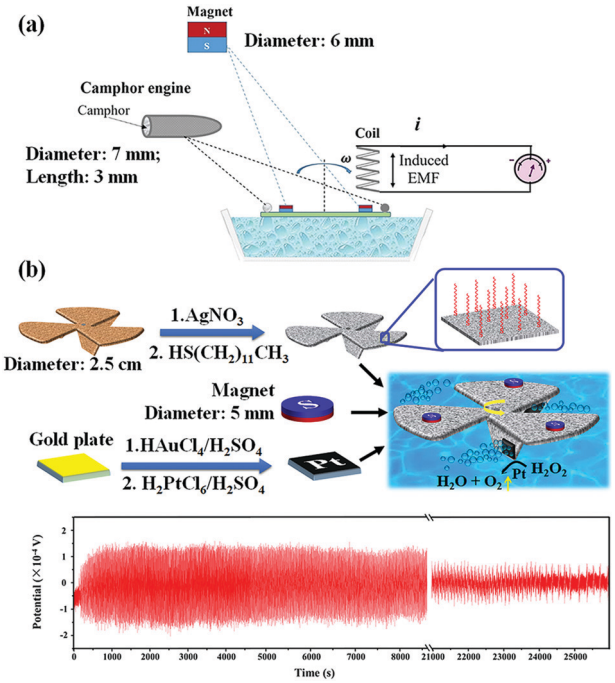

Fig. 5 (a) Schematic illustration of the self-propulsive mini-generator based on the camphor engine; adapted with permission from ref. 24. Copyright 2019 American Chemical Society. (b) The self-propulsive mini-generator based on the bubble-driven rotator and the generated electricity. Adapted with permission from ref. 44. Copyright 2016 American Chemical Society.

miniaturized size, gravitational force could easily result in the diving process once the device density is larger than that of water. Therefore, the research focus is mainly on developing driving forces for surfacing and re-diving strategies. The most widely applied method is inducing bubbles into the smart device to reduce the density for surfacing. Earlier, we incorporated a platinum catalyst in a device to trigger the chemical decomposition of hydrogen peroxide, which generates oxygen bubbles within the device and decreases the total density for surfacing; after rising to the water/air interface and connecting to the atmosphere, the bubbles are released and the re-diving process is realized.[16] Based on this principle, a reciprocating diving/surfacing motion could be realized for self-propulsive mini-generators *via* vertical motions.[19] Recent progress has elaborated several stages including (1) early efforts on applying chemical reactions to generate bubbles, (2) directly using bubbles to reduce energy dissipation in chemical reactions such as heat loss, and (3) combining such mini-generators to applicable scenarios for practical uses.

Mini-generators driven by chemical reactions. Chemical reactions that release gas bubbles were applied earlier in mini-generators based on vertical motions due to the feasible adjustment of density fluctuation *via* the bubbles. In 2014, both Chattopadhyay *et al.*[18] and our group[19] reported the use of chemical reactions to release bubbles as the driving force of vertical motions. At the microscale, Chattopadhyay *et al.* designed a micro bot consisting of a resin bead (diameter: ~900 μm) deposited with Pd nanoparticles as catalysts and attached with a micro magnet (Fig. 6a).[18] They placed this micro bot in a glass tube coiled with copper wire in the centre part and filled with H_2O_2 solution and a top layer of dyed alcohol; the micro bot underwent periodic vertical motions by breaking the bubbles upon touching the alcohol layer to increase the density for diving, gathering the bubbles *via* the decomposition reaction of H_2O_2 with the release of oxygen bubbles to gain extra buoyancy for surfacing. For such a microscale system, the directly generated electrical energy is quite low (Fig. 6b); therefore, they used two-stage amplification to obtain an induced voltage in the millivolt range.

At a macroscopic scale in the millimetre to centimetre range, we designed a functionally cooperative system integrated with a device made of porous copper foam containing magnesium, a smart surface as a pH-responsive switch, and a parallel magnetic field (Fig. 7a).[19] The as-prepared cubic device had a slight lower density than that of water and the smart surfaces were superhydrophobic to prevent solution infiltration. On changing to an acidic condition, the smart surface and the chemical reaction function cooperated by sequentially changing the surface wettability to superhydrophilic, allowing the acidic solutions to infiltrate and finally trigger the chemical reaction of Mg–HCl to release hydrogen bubbles. With the accumulation of bubbles, the device density increased and resulted in a surfacing process. When touching the air/water interface and releasing the bubbles, the device could realize diving/surfacing processes repeatedly. The reciprocating motions

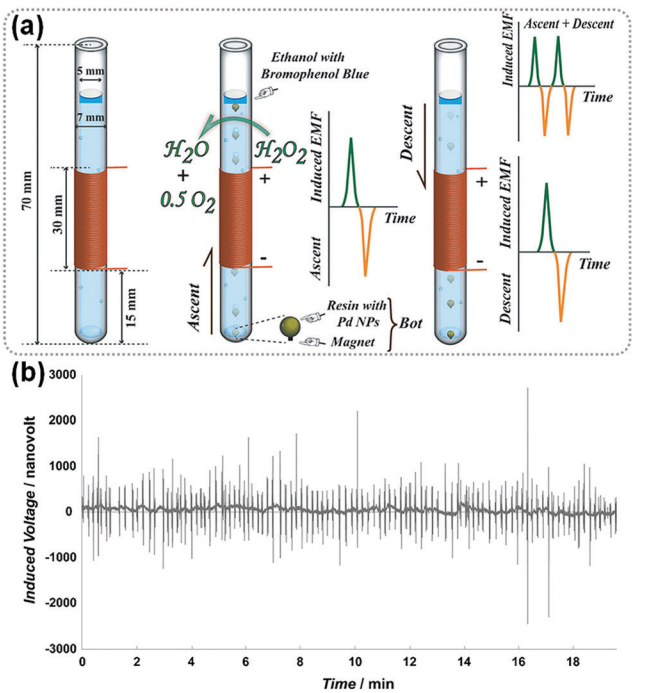

Fig. 6 (a) The surfacing/diving vertical motion of the micro bot in a glass tube. Each surfacing/diving motion generates an EMF signal as shown in the plots beside the tubes; (b) induced voltage generated from the motion of the micro bot. Adapted with permission from ref. 18. Copyright 2014 Wiley.

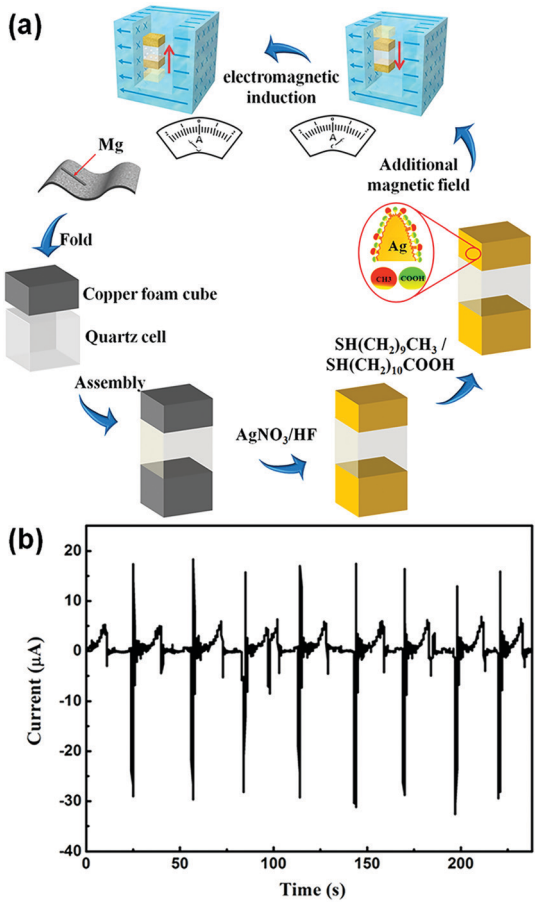

Fig. 7 (a) Schematic illustration of the fabrication process of the pH-responsive self-propulsive mini-generator; (b) induced current generated from the vertical motions. Adapted with permission from ref. 19. Copyright 2014 Wiley.

were exposed to a parallel magnetic field and induced a direct output current of about 20–30 μA (Fig. 7b).

Besides a directly observable output, the miniaturized mini-generator of centimetre size could also provide feasibility to improve the performance of self-propulsion and electricity generation by optimizing the related parameters. For example, improvements in the system design are effective for increasing the output by one magnitude and the energy conversion rate was increased by three magnitude.[86] The optimization includes the use of a device geometry that is almost streamlined, replacing the smart surfaces by a combination of superhydrophobic and pH-responsive wettable surfaces and accelerating the chemical reactions. Apart from the chemical reactions of Pd/Pt–H_2O_2 and Mg–HCl that release oxygen and hydrogen bubbles, respectively, the reaction between $CaCO_3$ and HCl has been applied to generate chemically inert CO_2 bubbles for propulsion.[21] Even though chemical reactions that release bubbles are effective to realize vertical motions, the energy conversion rate is not satisfactory. This is because most of the energy such as heat dissipation is not used for energy conversion to kinetic energy and electrical energy. Basically, the dominant factor in reciprocating diving/surfacing is the slight density fluctuation. Therefore, avoiding energy dissipation should be possible to improve the conversion rate from input to output energy.

Mini-generators driven by pressure change. In nature, many bony fish can dive/surface and stay at different water depths without the instantaneous input of external energy. They mainly rely on the swim bladder organ, which is filled with gas and can contract/expand according to the ambient pressure. This biological process does not need mass transfer or exchange of gas but rather relies on the volume change of the gas, which is more sensitive and energy-economic. Inspired by this biological design, we designed a self-propulsive mini-generator based on pressure-responsive motions.[22] Instead of using chemical reactions, we directly loaded a bubble onto the superhydrophobic back of a 3D-printed fish, which is sealed in a container filled with water (Fig. 8a). The closed system is further connected to a pressure changing system and a sphygmomanometer to indicate the system pressure. The as-prepared 'fish' has a density (0.997 g cm^{-3}) that is slightly lower than that of water at ambient pressure; after increasing the system pressure by 40 Pa, the total density increased to 1.006 g cm^{-3} to cause the diving process; when changing the pressure back, the 'fish' surfaces back to the water surface (Fig. 8b). This pressure-responsive motion is rapid and sensitive similar to that of real fish because no mass transfer processes such as bubble gathering or release are necessary. Correspondingly, the mini-generator of this self-propulsive device reaches an energy conversion rate of 10^{-3}%, which is 2–5 magnitude larger than that of bubble propulsion cases.

The pressure-responsive mini-generators still need to be improved on two aspects: (1) high-grade mechanical energy is input as the energy resource; with the increasing demand in

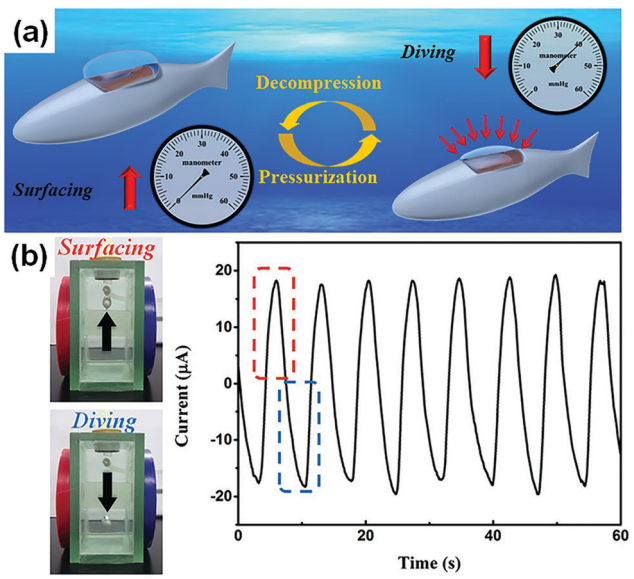

Fig. 8 (a) Schematic illustration of the pressure-responsive motion; (b) apparatus of the self-propulsive mini-generator and the induced current–time curve during vertical motions. Adapted with permission from ref. 22. Copyright 2017 Wiley.

energy diversity, harvesting energy from the environment is an attractive advantage of mini-generators; (2) human intervention is required to change the system pressure; therefore, a 'smarter' functionally cooperating system remains to be developed. To address these issues, we designed a mini-generator that could harvest sunlight energy and actively change the device density based on the photothermal effect.[23] To be specific, the photo-induced mini-generator has a black superhydrophilic device to hold the bubbles, a quartz window to collect light energy, a superhydrophobic part to reduce fluidic drag, and a permanent magnet to produce varied magnetic field (Fig. 9a). These components function in a cooperative manner under natural sunlight: when the device is at the bottom of the container with the quartz window directly facing the focused sunlight, light energy, having passed through the window, is converted into heat and the temperature of the black device increases due to the photothermal effects; meanwhile, the bubble within the device expands and provides extra buoyancy to the device for surfacing; when rising up to the water surface, the device gradually cools down to result in the contraction of the bubble and declined device density for re-diving; once the device dives to the bottom facing the focused sunlight again, a new surfacing/diving cycle starts (Fig. 9b). This photo-induced mini-generator has a direct induced voltage of 1.6 V when the focused sunlight has a power of 6.4 W (Fig. 9c). More importantly, the input of high-grade energy is not necessary but natural sunlight in winter is sufficient; no human intervention is necessary to change the system pressure but the integrated systems could realize the density fluctuation automatically. Taken together, such self-propulsive generators hold promise for developing energy-economic strategies of energy conversion for the power supply of micro-electronics.

4.3 Self-propulsive mini-generators *via* other motions

Besides the regular motions of horizontal rotation and vertical diving/surfacing movements, other forms of self-propulsion have been applied to design mini-generators, such as 'drinking bird' with reciprocating motions and actuators consisting of helical structures with reversible torsional movements in response to stimuli. The basic principle of these mini-generators is the integration of self-propulsion with varied magnetic fields to produce induced current in the circuits.

'Drinking bird' mini-generators. 'Drinking bird' is a toy heat engine mimicking a bird drinking water repeatedly,[37–39] and therefore, was sometimes incorrectly referred to as a 'perpetual motion machine'. A drinking bird normally has two glass bulbs as the 'head' and the 'belly', which are joined by a glass tube with one end attached to the head and the other end connected to the belly (Fig. 10a). The head together with the 'beak' is wrapped with felt-like materials and a highly volatile liquid (*e.g.*, dichloromethane, CH_2Cl_2) is stored in the belly. The underlying propulsion mechanism is a thermodynamic cycle driven by a slight temperature difference that converts heat energy into pressure difference and mechanical work; once the bird starts 'drinking' water by dipping its beak into the water by the side, the absorbed water through the felt-like material gets wet and water evaporation lowers the temperature of the head; together with some CH_2Cl_2 vapor in the head condensing, a pressure drop occurs in the head, thus, causing the rise in the CH_2Cl_2 liquid in the warm belly; as a result, the centre of gravity moves up and causes tipping over of the head to drink water again; meanwhile, the CH_2Cl_2 liquid flows back to the belly due to an equal pressure of two ends, leading to a vertical position of the bird to start another cycle with evaporation on the head. This repeated motion could last for days driven by the thermodynamic cycle.

To quantify the motions of the drinking bird and to convert this kinetic energy into electrical energy, Lorenz designed a mini-generator system by attaching a magnet to the bottom of the belly and placing a coil below the belly (Fig. 10b).[37] When the

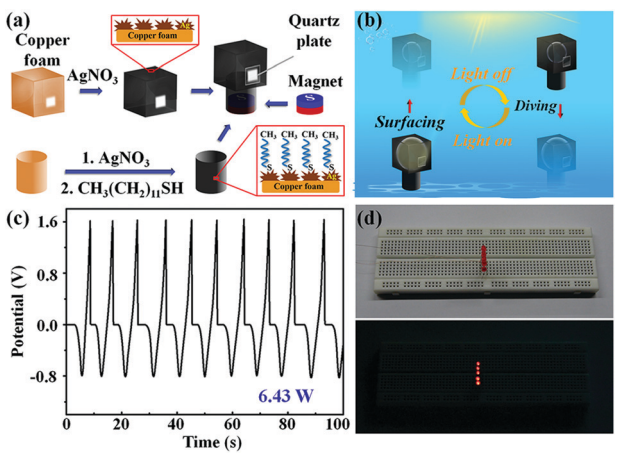

Fig. 9 Schematic illustration of (a) the fabrication of photo-induced mini-generator and (b) photo-responsive vertical motions; (c) induced voltage of 1.6 V under sunlight of 6.4 W and LEDs powered by the mini-generator. Adapted with permission from ref. 23. Copyright 2018 Wiley.

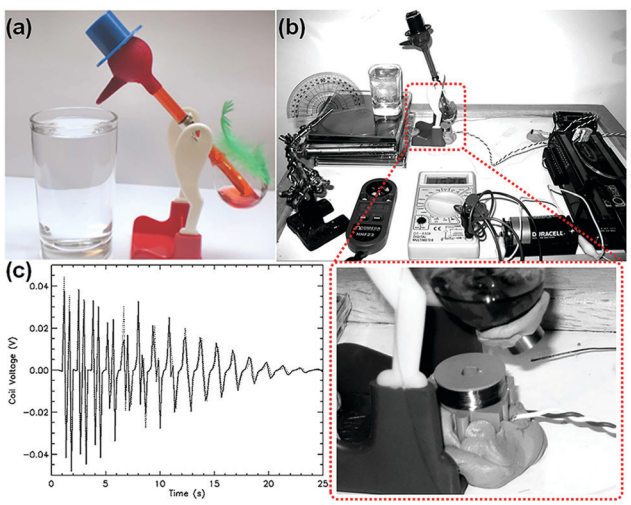

Fig. 10 Photographs of (a) a drinking bird and (b) the experimental setup of the mini-generator based on a drinking bird; (c) the induced voltage–time curve. Adapted with permission from ref. 37, Copyright 2006 AIP Publishing; from ref. 38, Copyright 2019 Scientific Research Publishing Inc.

magnet on the belly sweeps past the coil, it generates an electrical pulse with a direct peak voltage of 0.05 V and an average power output of 0.27 μW (Fig. 10c). The facile integration of normal materials makes the 'drinking bird' mini-generator a versatile solution for electricity generation, especially for poor areas without access to large facilities.

Mini-generators based on torsional/bending motions of actuators. Soft actuators consisting of twisted or deformable materials (*e.g.*, fibres) with responsive properties show fast and reversible torsional rotations or bending motions upon intermittent stimuli. Taking torsional actuators as an example, during the fabrication of these actuators with twisting processes, a large start-up torque was created; the stimuli that induces the deformation of the twisted fibres will trigger the rotation of the woven entity; on the other hand, removing the stimuli will recover the shape, thus leading to reversible motions and making electricity generation possible based on Faraday's law.[43,45,87–89] Diverse stimuli-responsive systems have been developed to demonstrate such torsional/bending motions for the application of artificial muscles,[90] soft robots,[1] valves, and mini-generators.[91] The demonstrated stimuli include solvent,[43,92] moisture,[45,93,94] and light[95,96] for materials such as carbon fibres, hydrogels, liquid crystalline, and *Bacillus* spores.

Solvent actuation. Inducing hierarchically helical structures in the preparation process, multiscale gaps may form between the helical components, thus allowing for the rapid diffusion of solvents or vapours. Together with the pre-twisted structures, deformation occurs in response to solvent/vapour favours for torsional motions. For example, Peng and co-workers helically assembled multiwalled carbon nanotubes into primary fibres and twisted them (Fig. 11a).[43] The nanoscale gaps between the nanotubes and micrometre-scale gaps between the fibres provide space for the fast transport of solvents (*e.g.*, ethanol, acetone, toluene, and dichloromethane). Because the fibres are sensitive to these polar solvents, contractive stress occurs rapidly within 0.5 s after applying the solvents. Owing to the volatile characteristics of these solvents, evaporation will induce recovery of the fibres, accompanied by reverse torsional rotation. Based on the fast rotations driven by the solvents, they constructed a mini-generator by integrating the fibre with a coil and a magnetic field (Fig. 11b). By converting the rotary kinetic energy into electrical energy, they obtained a peak current output of 0.11 mA (Fig. 11c).

To improve the energy conversion efficiency and output, Gao and co-workers fabricated hand-controlled actuators responding to polar solvents by programming hand-twisted fibres of graphene oxide, with mirrored helix configurations and hair-like diameter.[92] When stimulated by the polar solvent acetone, the graphene oxide fibres performed rapid rotary motion due to the oxygen-rich functional group with high affinity and rapid diffusion of polar molecules. Untwisting occurs upon solvent diffusion and recovery is realized after the evaporation of these solvents. By combing twisted units of different configurations, they improved the kinetic-to-electrical energy conversion rate to 54% and reached a peak power output of 89.3 W kg^{-1}.

Moisture actuation. Unlike the solvent, water and moisture are mild and environment-friendly stimuli for triggering reversible torsional rotation. Moreover, moisture-driven actuation is biocompatible and promising for integration with bio-species and is applied in wearing devices. To realize moisture-activated torsion, Qu *et al.* fabricated a graphene-fibre actuator by rotating the freshly spun graphene oxide (GO) hydrogel fibre along the axis.[45] Due to the oxygen-rich functional groups of GO, the GO layers reversibly expand/contract through the adsorption and desorption of water molecules (Fig. 12a). As a result, the formed helical geometry of GO fibres would enable reversible torsional rotation with a maximum rotation rate of 5190 rotations min^{-1} under the variation of humidity. On the

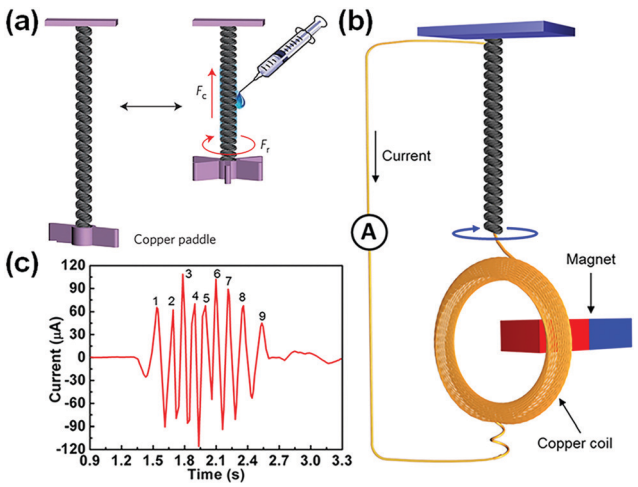

Fig. 11 Schematic illustration of (a) the torsional rotation of fibres when applying a solvent and (b) the construction of the mini-generator based on the fibre actuator; (c) induced current–time curve. Adapted with permission from ref. 39. Copyright 2015 Springer Nature.

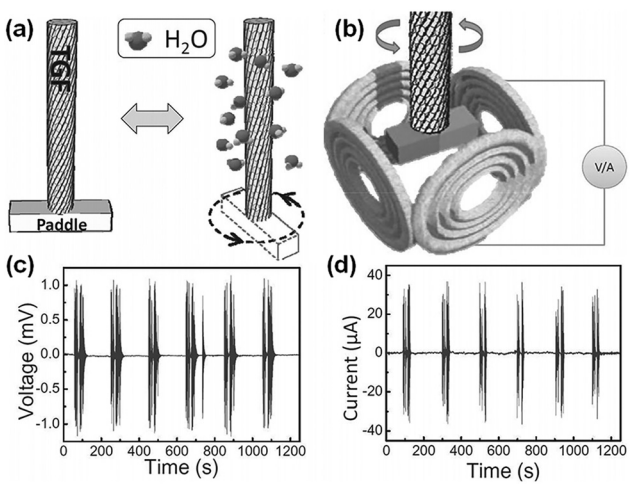

Fig. 12 Schematic illustration of (a) the rotation motion of GO fibres at low (left) and high (right) humidity and (b) the fabricated mini-generator; induced (c) voltage and (d) current generated by the mini-generator. Adapted with permission from ref. 45. Copyright 2014 Wiley.

basis of fast rotation motions, they constructed a mini-generator by attaching a magnet bar at one end of the twisted GO fibre and placing it at the centre of the coils, which can generate a voltage of 1 mV and a current of 40 μA (Fig. 11b–d).

Owing to the biocompatibility of moisture-driven rotation, a wearing apparatus is possible depending on the large-scale accessibility and mechanical flexibility of such mini-generators. To this end, Yuan and co-workers took inspiration from helical microfibrils in plant cells and fabricated a hygroscopic cloth actuator by impregnating a commercial cloth template with a 3D nanoporous hybrid network of polymer/carbon nanotubes.[97] In response to drying/wetting, the cloth actuator contracts and expands along with the desorption and adsorption of water in the helically arranged microfibers, respectively (Fig. 13a). Furthermore, the nanoporous structures allow for the feasible diffusion of water through the actuator. By further integrating fibre rotation with a magnet and a coil, they fabricated a cloth actuator-based mini-generator with a high induced voltage of 75 mV (Fig. 13b). Similarly, Wang and co-workers fabricated an actuator of twisted gel-state natural alginate fibre *via* a wet spinning process.[98] Due to the good moisture-responsive properties, the twisted fibres could swell and contract reversibly, leading to a rapid rotational motion with a speed of 13 000 rpm. By further integrating the rotations with a magnet and a solenoid, they fabricated a mini-generator that produced a maximum voltage of 2.8 V after amplification.

In nature, moisture actuation is found to drive bending motions. For example, *Bacillus* spores are a type of dormant cells that can swell and contract with a diameter change of about 12% in response to humidity change. Sahin and co-workers created a thermodynamic cycle of *Bacillus* spores by adjusting the force and relative humidity with an AFM machine, and found an energy density of more than 10 MJ m^{-1}.[94] They doubled the energy density by assembling the spores into dense, submicrometre-thick monolayers on a silicon micro-cantilever and elastomer sheets (Fig. 14a).[93] The bio-hybrid actuator displays periodical bending motion for 1 million cycles. Based on the bending motion, they integrated a spore-coated rubber with an electromagnetic generator having an open container of water by its side (Fig. 14b); when alternately changing the moist streams of air, the magnet was driven back and forth by the vibration of the spore-based sheet to induce a current in the circuit. The average output power was about 0.7 μW and the electrical power was about 233 mW kg^{-1}.

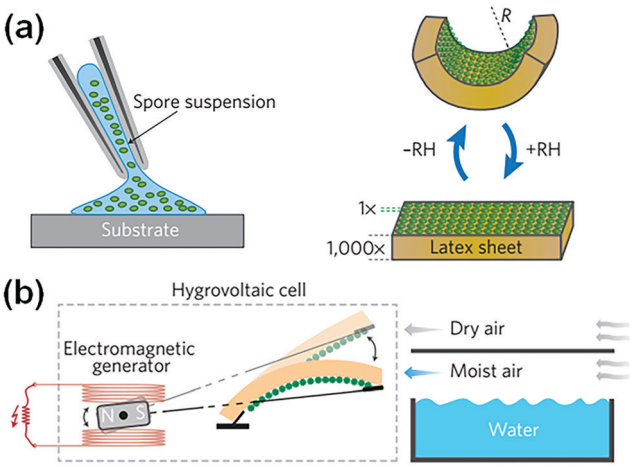

Fig. 14 (a) Schematic illustration of the assembly of the spore on a latex sheet and the bending motion of the actuator; (b) apparatus of the mini-generator based on the spore actuator. Adapted with permission from ref. 93. Copyright 2014 Springer Nature.

Thermal actuation. Low-grade waste heat exists in industrial waste streams, automobiles, power plants, *etc.* Developing a feasible strategy for harvesting this low-grade energy and converting it to electrical energy is meaningful. To this end, Kim and co-workers fabricated a thermally-powered rotary actuator by using the inexpensive, highly-twisted fishing line or sewing thread (Fig. 15a).[99] Anisotropic thermal expansion in twisted muscle fibre causes length contraction and correspondingly increases the fibre diameter on heating, leading to the untwisting motion. Then, they placed a magnetic rotor at the midpoint of the two segment fibres with the same/opposite handed configurations (Fig. 15b). Upon heat stimulus on either one or both of the segments, torsional rotation is triggered with reversibility in response to fluctuating air temperature, leading to induced signal on a miniature wire coil (Fig. 15c). With resonant temperature fluctuation at 19.6 °C, the mini-generator has an output power of 124 W kg^{-1}.

Light actuation. Azobenzene-containing polymers are known to exhibit photomechanical effect, which can convert light

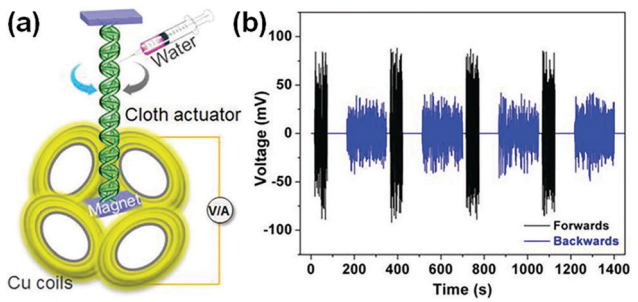

Fig. 13 (a) Schematic illustration of mini-generators based on hygroscopic cloth actuator; (b) induced voltage up to 75 mV produced by the mini-generator. Adapted with permission from ref. 97. Copyright 2017 Wiley.

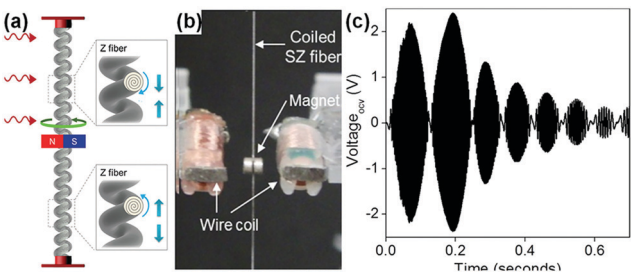

Fig. 15 (a) Schematic illustration of the untwisting and rotation motion of the top half of the torsional fibre during heating; (b) photograph of the mini-generator; (c) induced voltage up to 2 V. Adapted with permission from ref. 99. Copyright 2015 The Royal Society of Chemistry.

energy into kinetic energy *via* stimulus-responsive deformation such as bending, twisting, and contraction. To realize continuous output of kinetic energy *via* the oscillation of these photoactive materials, Yu and co-workers[95] designed a cantilever casted with azobenzene liquid-crystalline polymer on a substrate of grooved low-density polyethylene, wherein the cantilever showed rapid bending/unbending in response to UV exposure. They further attached copper coils onto one free end of the cantilever and exposed the bending motions in a magnetic field (Fig. 16a); along with the cantilever swinging and passing by the UV light, a current was induced in the coil based on the electromechanical principle (Fig. 16b).

Compared with UV light, near-infrared (NIR) light is more favoured in biomedical applications regarding biocompatibility. Yang *et al.* designed an NIR-driven polymer oscillator by selectively coating polydopamine on certain portions of the splay-aligned liquid crystalline network film (Fig. 16c).[96] As a result, this oscillator underwent a reversible bending motion: when NIR irradiation was applied on the portion selectively coated with polydopamine, the photothermal effects of polydopamine cause bending of the film; under the bent state, the uncoated portion of the film just blocks the NIR irradiation, thus cooling down the polydopamine portion; after cooling down and the film coming back to the original position, NIR irradiation is again applied to the polydopamine region to trigger another bending cycle. Furthermore, they applied focused sunlight irradiation to induce fast and steady oscillation of the film, which was converted into electrical energy by hanging coils to a string hit by the film near a magnet (Fig. 16d). The motion of string driven by the oscillation of the film could induce open-circuit voltage.

4.4 Applicable scenarios of self-propulsive mini-generators

When it comes to practical applications of mini-generators, the problem of consuming relatively high-grade energy but only to obtain a low output is to be urgently addressed. One possible solution to this problem is integrating mini-generator systems to applicable scenarios both by harvesting low-grade environmental energy from these scenes and supply power back to them.

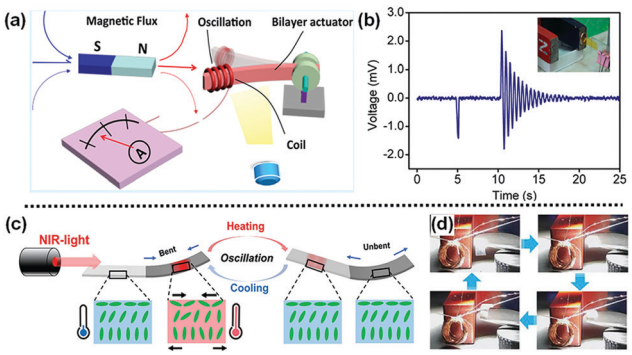

Fig. 16 (a) Schematic illustration of the mini-generator based on the UV-responsive bending motion; adapted with permission from ref. 95. Copyright 2015 American Chemical Society. (b) Induced voltage of the mini-generator; (c) mechanism of the NIR-light-driven oscillation motion of the NIR-responsive film; (d) apparatus of the NIR-driven mini-generator. Adapted with permission from ref. 96. Copyright 2020 Wiley.

One applicable scenario of self-propulsive mini-generators is harvesting energy from human activities for conversion into electrical energy to power some implanted electronics. This is because the energy stored in physiological activity is normally hard to collect *via* traditional methods; meanwhile, implanted electronics only consume low power such as a cardiac pacemaker (8–10 μW). To this end, we have integrated the self-propulsive mini-generator in response to pressure change of the periodic physiological change in the systolic/diastolic blood pressure.[36] The self-propulsive part is an *in vitro* cylindrical superhydrophilic device captured with a bubble in its empty interior wrapped with coil at the outside; this part, together with a fixed magnet, was immersed in water in a sealed container (Fig. 17). A slight pressure change of about 40 mmHg was sufficient to cause density fluctuation of the device to realize a reciprocating motion relative to the magnet and to generate electricity in the circuit. In particular, this pressure difference is in the range of human systolic/diastolic blood pressure difference. Therefore, we connected the sealed system to the femoral artery of a sheep's left leg; the heart-beating rhythm of the sheep is close to that of a human. A rhythmic blood pressure change, along with the heart-beat, could realize diving/surfacing cycles and induced voltage of about 0.3 V. With future minimization and encapsulation techniques, this proof-of-concept implanted mini-generator could harvest kinetic energy from the human body and apply the generated electricity back to supply implanted electronics, such as cardiac pacemakers, thus avoiding the surgery for replacing the battery.

Another applicable scenario of self-propulsive mini-generators is the integration with industrial fermentation processes, which generates gas products. Considering that the gathering and release of bubbles could propel vertical motions, we combined

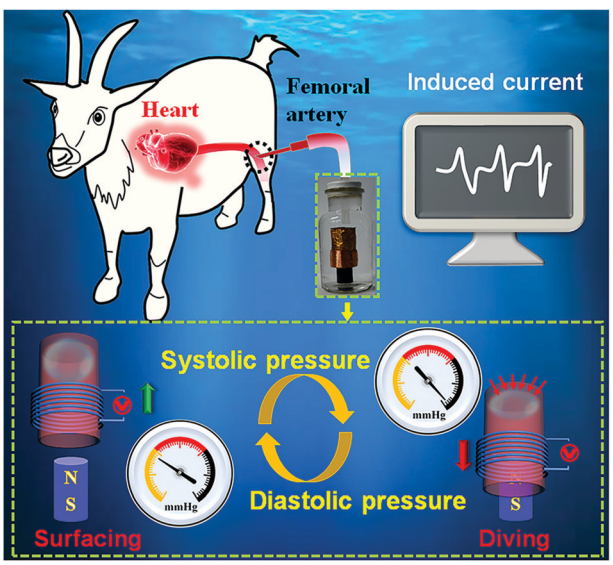

Fig. 17 Schematic illustration of the blood pressure-responsive mini-generator system. Adapted with permission from ref. 36. Copyright 2019 Wiley.

the fermentation production line with self-propulsion by passing the produced gas mixture through the device (Fig. 18a and b).[72] This integration design includes the bubble resource, a dark fermentation starch containing *Bacillus* sp. and *Brevundimonas* sp., which release hydrogen and carbon dioxide, a superhydrophobic valve to collect the generated bubbles, and a moving device loaded with magnets and covered with a superhydrophobic cone tip. When the gas bubbles released from the fermentation processes accumulated to the maximum holding capacity of the superhydrophobic valve, a large gas bubble escapes from the valve to the moving device; with declined density, the device surfaces to the air/water interface and releases the bubble through the superhydrophobic cone tip. The mini-generator achieves a maximum voltage of 2.4 V with a lifetime over 20 000 s to light a dozen red LEDs and shows an energy conversion efficiency of 40%. With the above integration, weak and low-grade internal energy of gas was collected but the gas only passes through without any loss. Therefore, the fermentation process is not disturbed and the production amount is not affected. Moreover, integration with a mini-generator harvests extra electrical energy, which has been used to power gas flowmeters of the fermentation line (Fig. 18c).

4.5 Hybridization of self-propulsive mini-generators with TENG

With different design principles, self-propulsive mini-generators and TENG show complementary characteristics: the former has a relatively high induced current based on Faraday's law, while the latter shows a high voltage with a large resistance based on the triboelectric effect and electrostatic induction. It could be anticipated that a hybridization of these two kinds of mini-generators could improve the total output, which holds promise to facilitate and broaden the applications of mini-generators. Until now, the demonstrated hybridized examples have used diverse energy resources including vibration/biomechanical energy, air flow/wind energy, and 'blue energy (energy stored in water waves)'.

Hybridized mini-generators harvesting vibration/biomechanical energy. To use the common but weak energy in vibrations, Wang and co-workers fabricated a hybrid cell by integrating TENG with self-propulsive mini-generators into a suspended structure (Fig. 19a).[100] The suspended structure is based on two oppositely oriented magnets, which can oscillate vertically around a balance point generated by its gravity and the repulsive force in response to external vibration. During oscillation, the friction layers attached on the surface of the suspended structure achieved a relative sliding motion that makes TENG work (Fig. 19b). At the same time, magnetic flux through the solenoid coil wrapped on the outer cube changed due to the up/down motion of the magnet, thus producing induced electricity. The hybridization of TENG and the electromagnetic generator results in an output voltage of 4.6 V and an output current of 2.2 mA in a parallelly-connected circuit.

In addition to vibration in the environment, periodic physiological activities of human beings, such as heartbeat, muscle stretching, and walking, could also be harvested by hybrid mini-generators. For example, Yang *et al.* combined TENG with six electromagnetic generators to harvest the motions of a wearer's wrist for the power supply of an electronic watch.[101] They placed a magnetic ball that could freely move within an acrylic box and pasted six coils on all the surfaces of the box to form an electromagnetic generator; meanwhile, the TENG was constructed at the bottom of the box consisting of a nylon film on a copper electrode and a transparent composite film of polyvinylbutyral nanowire/polydimethylsiloxane (PDMS) on another copper electrode (Fig. 20a). This watch-like hybrid

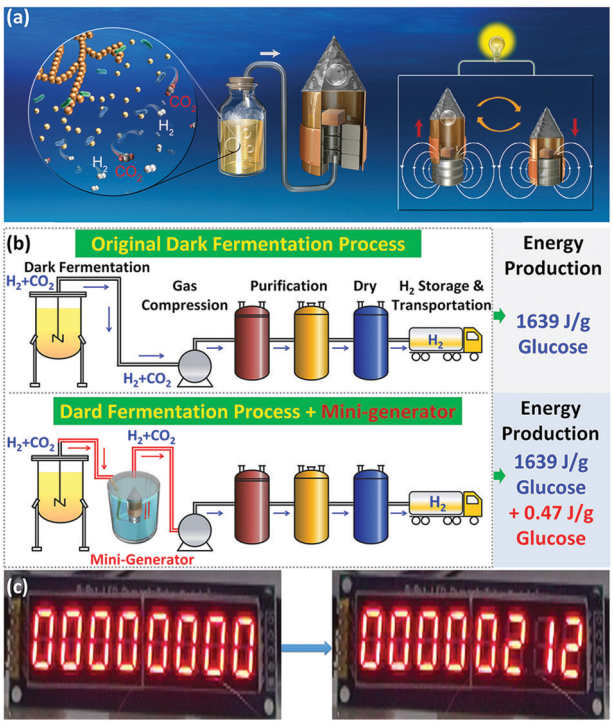

Fig. 18 (a) Integration of the self-propulsive device with fermentation processes; (b) production of industrial dark fermentation lines without and with the mini-generator; (c) the gas flowmeter powered by the mini-generator. Adapted with permission from ref. 72. Copyright 2019 Wiley.

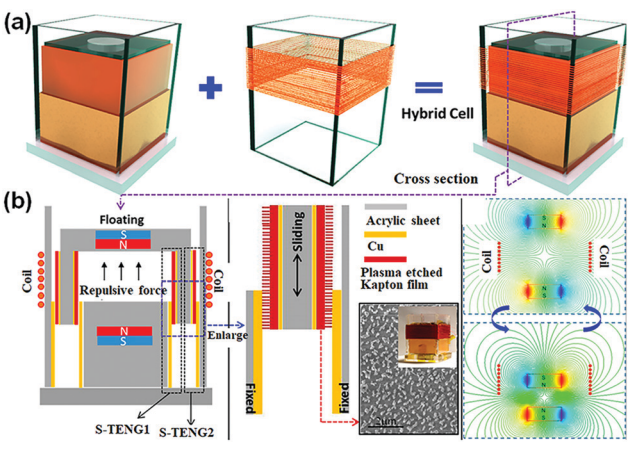

Fig. 19 (a) Schematic illustration of the hybridized mini-generator for vibration energy harvesting; (b) cross section view of the mini-generator and the simulated magnetic field distribution. Adapted with permission from ref. 100. Copyright 2014 American Chemical Society.

mini-generator collected vibration in wrist movements by collision between the magnetic ball and the walls of the acrylic box, which induces work of both the TENG and the electromagnetic generator. To extend energy conversion from human walking to electrical energy, they further fabricated an electromagnetic–triboelectric nanogenerator with the combination of a magnet, coils, triboelectric materials, electrodes, and springs.[102] The layers of acrylic substrates were separated by four springs from four corners; at the bottom substrate, they sequentially attached a permanent magnet, a buffer film, an aluminium film as the triboelectric material, and an electrode of TENG; at the top substrate, they assembled layers of a coil, a buffer film, an aluminium film, and a PDMS film (Fig. 20b). When the two substrates were pressed by external force in human walking, TENG functions in the contact-separation processes; meanwhile, the movements also cause a change in the magnetic flux and induced current in the coil to make an electromagnetic generator work. They mounted the hybrid generator in the heel of shoes to light up all the on-shoe LEDs.

Hybridized mini-generators harvesting air flow/wind energy. Air-flow/wind energy is highly attractive owing to its clean, renewable, and abundantly available sources in nature and environment. Harvesting wind energy in cities such as in tunnels and further converting into electrical energy to power detectors/sensors represents practical applicable scenarios of hybrid mini-generators.[103–105] On this aspect, Wang *et al.* demonstrated a self-powered wireless traffic volume sensor based on a rotating-disk-based hybridized mini-generator consisting of a rotator and a stator.[104] As shown in Fig. 21a, the whole device holds a disk structure composed of a rotator and a stator. The rotator has four crossed acrylic blades anchored on a disk-like acrylic plate; between the blades and the substrate lie three sequential layers of aluminum, polytetrafluoroethylene, and polyurethane, which are divided into four portions; the adjacent portions are inserted with rotating bar magnets and coils anchored on the bottom stator. Upon wind blowing resulting in the spinning of the rotator, relative sliding between the triboelectric materials make TENG function; at the same time, the relative movements between the magnets and coils could induce a current. With a rotation speed of 1000 rpm, the hybridized mini-generator output an instantaneous power of 17.5 mW for practical uses. The further integration with a commercial traffic volume sensor allows for harvesting air flow/wind energy from a tunnel (Fig. 21b), while monitoring real-time traffic volume.

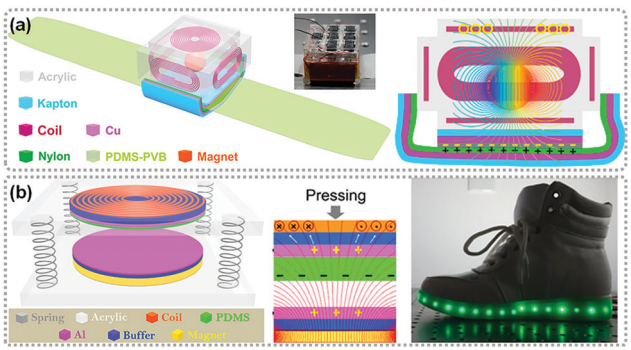

Fig. 20 (a) Schematic illustration of the fabrication and the working principle of the watch-like hybridized mini-generator; adapted with permission from ref. 101. Copyright 2015 American Chemical Society. (b) Function mechanism of the mini-generator when embedded into shoes during human walking. Adapted with permission from ref. 102. Copyright 2015 American Chemical Society.

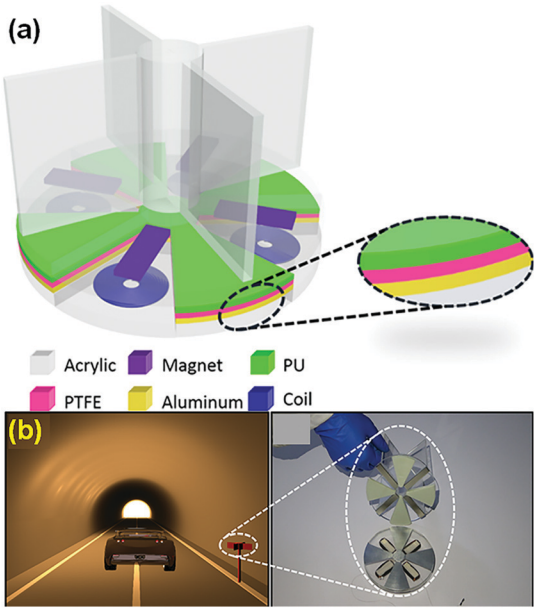

Fig. 21 (a) Structural design of the wind-driven hybridized mini-generator; (b) schematic illustration of harvesting wind energy in the tunnel and the photograph of the mini-generator. Adapted with permission from ref. 104. Copyright 2016 American Chemical Society.

To improve the output performance by changing the common rigid-to-rigid contact of triboelectric materials into soft and elastic contact, they fabricated an ultra-low-friction hybrid generator by replacing four elastic blades made of polymer thin films;[105] four arc-shaped magnets and copper foils were attached on the inner walls of the stator. The magnets and coils form an electromagnetic generator while the polymer films and the copper foils form a TENG. Rotation driven by wind at 1000 rpm led to a maximal load voltage of 65 V and power of 438.9 mW kg^{-1} for TENG, and a maximal voltage of 7 V and a power density of 181 mW kg^{-1} for the electromagnetic generator.

Hybridized mini-generators harvesting blue energy. Blue energy, such as tidal energy, current energy, and wave energy, is abundant in nature but difficult to harvest due to its low frequency and irregular amplitude. One solution is the combination of TENG harvesting low-frequency energy and an electromagnetic generator that collects high-frequency energy. To this end, Wang's group designed a hybrid mini-generator made from three coaxially placed cylindrical tubes with the inner and middle tubes capable of rotating or moving (Fig. 22a).[106] To construct a TENG, they coated the inner tube and the middle tube with triboelectric materials of copper and a fluorinated ethylene propylene (FEP) thin film in a spirally interdigitated manner. To integrate the electromagnetic generator, they attached

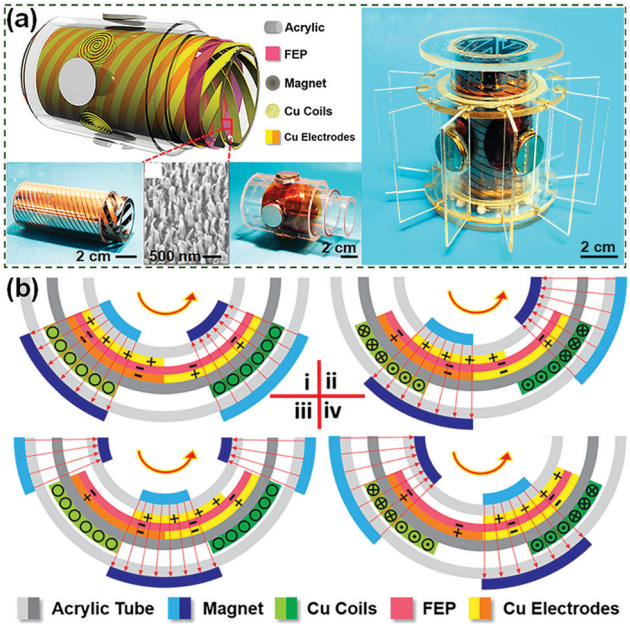

Fig. 22 (a) Structural design and (b) working mechanism of the hybridized mini-generator for harvesting blue energy. Adapted with permission from ref. 106. Copyright 2016 American Chemical Society.

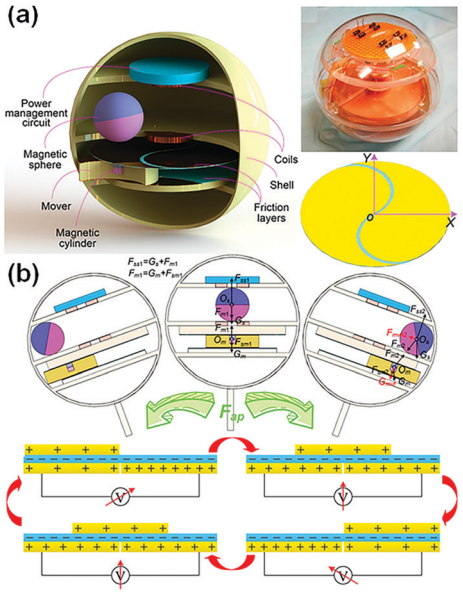

Fig. 23 Schematic illustration of (a) the structure and (b) working principle of the hybridized mini-generator for harvesting water wave energy. Adapted with permission from ref. 107. Copyright 2019 American Chemical Society.

four pairs of magnets both on the inner and outer tube while the coils were embedded on the middle tube. In addition, rotor blades were mounted on the outer tube to collect the flow energy. Taken together, during ocean tide, flow, or wave that causes the relative motions of the tubes, the TENG could harvest rotational (<100 rpm, <2 Hz) or translational energy by either sliding or pressing *via* the inner/outer magnetic attraction; meanwhile, the electromagnetic generator could harvest both rotation and fluctuation (>10 Hz) due to the magnetic flux change (Fig. 22b).

To minimize the size of the hybrid mini-generator to harvest blue energy, the same group fabricated a spherical shell with four inner zones divided by acrylic discs.[107] One magnet sphere was placed on the second top layer to move freely on the application of external forces (Fig. 23a). Two coils were embedded into two acrylic discs, which sandwiched the magnetic sphere, thus leading to an electromagnetic generator. The TENG was fabricated by placing a mover embedded with a magnetic cylinder and coated with copper films between the bottom two acrylic layers. During waves, the magnetic sphere moves to provide a variable magnetic flux to induce electricity and meanwhile, drives the mover to slide between the friction layers and be attracted to press the layers, both generating electricity based on the TENG principle (Fig. 23b). As a result, the hybridized generator is capable of capturing blue energy to power wireless sensor networks or to monitor environmental conditions, such as temperature and pH.

5. Other applications of functionally cooperating systems

To date, the applications of functionally cooperating systems have mainly focused on self-propulsive devices, which are further used in the research fields of mini-generators, self-assembly, directed transportation, *etc.* The motion pattern differs depending on the targeted end uses. For example, regular reciprocating motions are essential to ensure the steady output of mini-generators. However, when mimicking the self-assembly of molecules at a visible length scale, a random motion may be required. Correspondingly, the design of functionally cooperating systems varies according to specific applications.

Macroscopic supramolecular assembly (MSA)

In the research field of self-assembly, the concept of 'self-assembly at all scales'[108] has provided a vision of automatic organization of components at all length scales. For decades, research on self-assembly has mainly focused on microscale building blocks; recently, the development of 'macroscopic supramolecular assembly (MSA)'[109–112] has facilitated the possibility of assembling large building blocks with a size exceeding 10 μm by studying non-covalent interactions between macroscopic surfaces (Fig. 24). Unlike nanoscale components or molecules relying on molecular thermal motions for random movements, these macroscopic building blocks could hardly diffuse, collide, and interact without external propulsive forces.[113,114] Therefore, self-propulsive building blocks based on functionally cooperating systems provide a solution for the highly spontaneous assembly of macroscopic components similar to molecular self-assembly. The design of self-propulsive building blocks includes (1) loading of driving forces for random motions, (2) alignment of building blocks based on the principle of minimizing free interfacial energy, and (3) rapid molecular interactions between physically assembled surfaces. The reported works mainly include macroscopic assembly *via* physical interactions and MSA *via* molecular interactions.

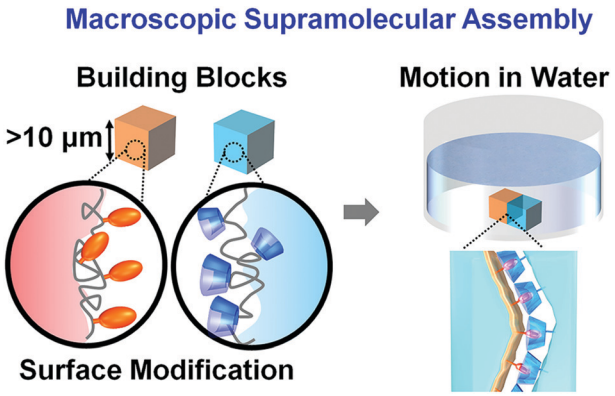

Fig. 24 Schematic illustration of macroscopic supramolecular assembly. Adapted with permission from ref. 113. Copyright 2020 Wiley.

Early work on macroscopic assembly *via* physical forces was demonstrated by Whitesides *et al.* They designed millimetre-scaled PDMS plates loaded with platinum to realize self-propulsion in a H_2O_2 solution by ejecting small gas bubbles in the catalytic decomposition of H_2O_2. Moreover, the thin plate shape allows for the floating of PDMS and the hydrophobic side surfaces generates negative menisci, which induces the overlap of the two PDMS upon their movement into the capillary length[65] (Fig. 25a). The attraction results from the minimization of free interfacial energy. These plate-building blocks could move automatically to form dimers *via* their hydrophobic surfaces. With the demand for increasing the assembled geometry and the size of the building blocks, we later designed centimetre-sized cuboid PDMS building blocks with anisotropic wettability. To enhance the driving force for the self-propulsion of these macroscopic components, we induced hierarchically rough structures of platinum, which resulted in the rapid release of oxygen bubbles upon contacting an H_2O_2 solution.[32] By varying the loaded side surfaces of rough platinum, we could tailor the 'growing sites' of the building blocks in the assembly: PDMS loaded with platinum on the opposite side surfaces form a line structure *via* the unmodified hydrophobic side surfaces; with platinum on the adjacent side surfaces, the building blocks form a triangle structure, allowing for the further 'growth' of the two 'arms' (Fig. 25b). Besides, a certain degree of human intervention could also direct the assembly based on capillary-induced assembly.[115]

The combination of self-propulsion and capillary force is effective for the formation of ordered structures at the interface; however, the collapse of these structures occurred when lifting them out of the interface without any post-stabilization methods. Therefore, we further integrated fast supramolecular interactions on the physically-assembled surfaces. This integration requires three key factors including (1) replacing the driving force to bubble-free systems because bubbles attach to the surfaces and hinder the compact combination of building blocks, (2) the conversion from assembly *via* hydrophobic surfaces to assembly *via* hydrophilic surfaces to further induce functional groups, and (3) rapid molecular interactions within a short contact process in a dynamic situation.

Correspondingly, we applied the Marangoni effect to replace the driving force due to Pt–H_2O_2 by loading the surfactants within the building blocks and slowly releasing them onto water (Fig. 26a).[33] To make the menisci of hydrophilic surfaces dominant in the assembly, we adjusted the PDMS density at the water/oil interface; with growing density, the hydrophilic menisci gradually grew larger than the hydrophobic menisci, thus leading to assembly *via* hydrophilic surfaces (Fig. 26b). Based on this hydrophilic assembly, we further developed a strategy for fast molecular interactions between the macroscopic

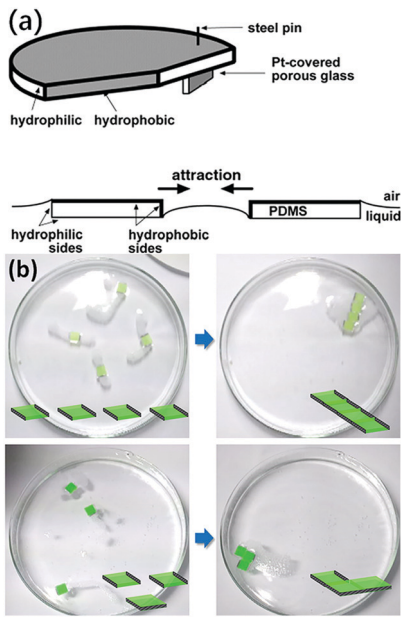

Fig. 25 (a) Design of PDMS plates for self-propulsion and assembly *via* capillary attraction. Adapted with permission from ref. 65. Copyright 2002 Wiley. (b) MSA patterns of line or triangle structures directed by anisotropic modification. Adapted with permission from ref. 32. Copyright 2014 Wiley.

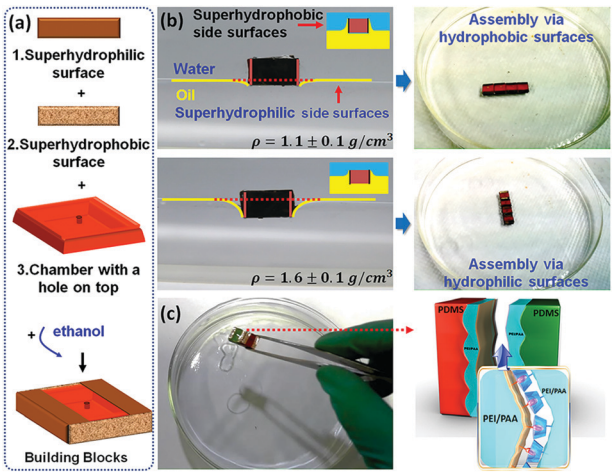

Fig. 26 (a) Design of Marangoni-effect-driven building blocks; (b) conversion of assembly *via* hydrophobic surfaces to hydrophilic surfaces; (c) fast interfacial assembly facilitated by a compliant surface coating. Adapted with permission from ref. 33. Copyright 2015 Wiley.

surfaces by pre-coating a highly compliant surface, termed as a flexible spacing coating.[116–119] Such coatings could be fabricated by a facile layer-by-layer assembled technique.[120–122] The coatings could increase the molecular motility for multivalency and thus enhance the interfacial binding forces. Within short contact or collision in self-propulsion, these centimetre-sized PDMS could be assembled *via* molecular recognition and lifted out of the interface immediately after assembly (Fig. 26b).

Due to the advantages in the flexible design of building blocks, the self-propulsion process could be tailored over moving velocity, lifetime, *etc.* For example, for the Marangoni-effect-driven self-propulsion *via* the releasing surfactants, the surface tension gradient could be changed by constructing competitive equilibria of surfactant absorption and dissolution *via* supramolecular recognition (Fig. 27a).[34] The release and absorption rate of the surfactant molecules at the air/water surface determines the surface tension valley, while the capture and dissolution rate of the surfactants *via* the host molecules in water ensures the recovery rate of the high-surface-tension area. The relative rates determine the surface tension gradient and the lifetime of motion. With optimized parameters, we increased the self-propulsion lifetime of the building blocks at a medium moving velocity (Fig. 27b), thus allowing for sufficient interaction and assembly chances. Finally, compared with the normal case with surfactants only, Marangoni self-propulsion assisted by the competitive equilibria could increase the assembly ratio of 60 parallel independent dimers from 20% to 100% (Fig. 27c).

Directed transportation

Owing to the spontaneous and integrative characteristics, the self-propulsion of functionally cooperating systems could realize complex missions such as directed transportation between different phases (*e.g.* oil/water) and active search/separation/collection of spilt oil. For example, the directional delivery of small molecules between different phases requires the integration of smart surfaces, self-propulsive devices, and

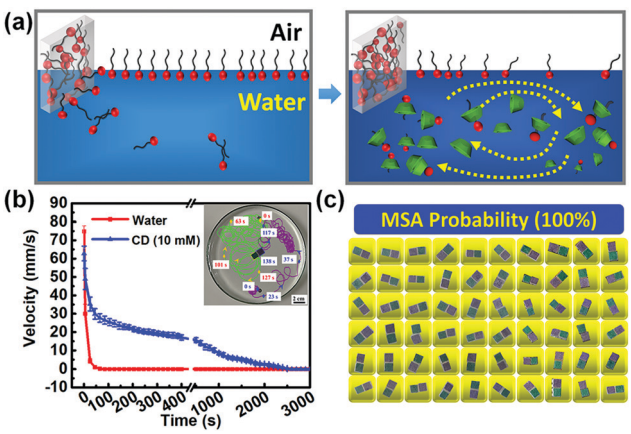

Fig. 27 (a) Prolonged Marangoni effect *via* the strategy of supramolecular recognition; (b) comparison of self-propulsion lifetime with (CD solution) and without (water) supramolecular recognition; (c) photos of 60 parallel MSA assembled dimers. Adapted with permission from ref. 34. Copyright 2018 Wiley.

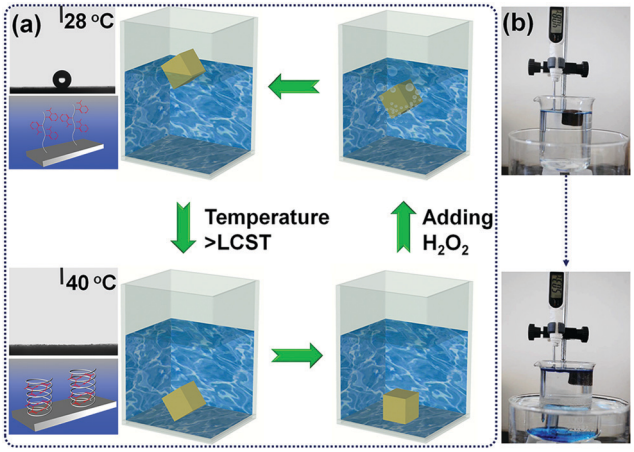

Fig. 28 (a) A diving-surfacing cycle *via* cooperating effects of thermally-responsive coatings and bubble propulsion mechanism integrated in the device; (b) directed delivery of small molecules between different phases. Adapted with permission from ref. 17. Copyright 2013 Wiley.

stimulus-responsive mechanism. We fabricated a functionally cooperative device of porous nickel foam loaded with platinum in the interior and coated with a rough gold structure and a coating of thermally-responsive poly(*N*-isopropylacrylamide) (PNIPAAm) (Fig. 28a).[17] The device was used to deliver lipophilic molecules between the two oil phases of hexane and carbon tetrachloride separated by a water phase with the following procedure. In the beginning, the device floated at the interface of hexane/water at 40 °C and absorbed the lipophilic oil molecules within the hexane phase due to the porous superhydrophobic surfaces. After cooling down to 28 °C, the configuration of PNIPAAm changed from a shrunken dehydrated state to a swollen hydrated state, which further caused a wettability change in the device to superhydrophilic. With the infiltration of water into the device and an increased density, the device dived to the bottom of the water/CCl_4 interface to release the loaded dye molecules into the CCl_4 phase (Fig. 28b). The cooperative effects of thermally-responsive diving-surfacing motions, wettability change for selective permeability of small molecules, and density fluctuation of the device made the directional delivery possible.

In the horizontal direction, the self-propulsion of functionally cooperating systems was applied for the active clean-up of spilt oil. In most oil spill cases, conventional passive methods mainly include the steps of gathering oil *via* fencing, absorption, and separation of oil from water. Self-propulsive devices could integrate these functions with an active feature. For example, Guan *et al.* fabricated a self-propelled Janus foam motor loaded with camphor/stearic acid, which provided driving forces *via* the Marangoni effect on water (Fig. 29a).[71] The millimetre-scaled sponge-like device moved randomly on the water surface and attracted oil droplets *via* capillary effects. To increase the oil loading capacity, we designed a boat-shaped device consisting of a propulsion system (both Pt–H_2O_2 and Mg–HCl are applicable) to 'search for' spilt oil by spontaneous motions, superhydrophobic/superoleophilic surfaces to collect dispersive oil, and a reservoir to store/release gathered oil (Fig. 29b). The active

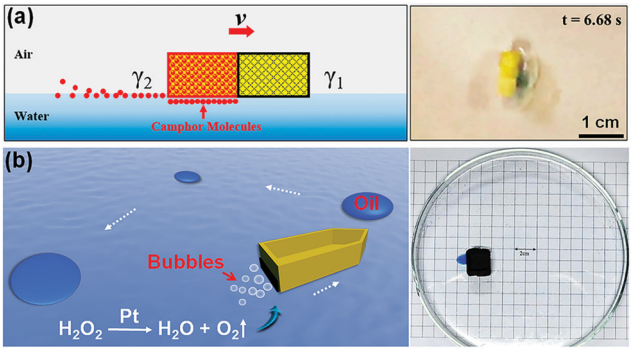

Fig. 29 (a) A self-propelled Janus foam driven by the Marangoni effect to absorb oil on water; adapted with permission from ref. 71. Copyright 2019 MDPI. (b) Active search/collect of spilt oil *via* a functionally cooperating system. Adapted with permission from ref. 35. Copyright 2019 Wiley.

working, macroscopic device size, and increased capacity together favour the continuous missions of search/capture/collect/unload of spilt oil.[35]

6. Summary and outlook

To summarize, we have introduced the progress of 'functionally cooperating systems' and demonstrated the underlying design principles for self-propulsion, which is further applied in advanced fields of mini-generators, macroscopic supramolecular assembly, directed transportation, *etc.* In particular, the progress in self-propulsive mini-generators has been emphasized with the vision of increasing the energy diversity for power supply of low-energy-consumption electronics. The integrative and cooperative characteristics of multiple materials and functions have become a growing trend in smart materials. Beyond the manufacture of materials with designated size, shape, and properties, functionally cooperating systems require the creative design of programmable processes between components to complete complex missions. Similar to a personal computer, the intelligence degree of artificial materials remains to be improved with future development on the aspects of miniaturization, increased complexity, systematicity, and programming features. We envision that functionally cooperating systems provide a proof-of-concept idea for the construction of smart systems from the designs of materials science and chemistry. It is also highly anticipated that further combinations with interdisciplinary sciences such as artificial intelligence, image recognition, and biological science will aid in the development of artificial systems for completing similar complex tasks in life science.

Conflicts of interest

There are no conflicts to declare.

Acknowledgements

We appreciate financial support from the National Natural Science Foundation of China (21674009; 21875017), the National Science Foundation for Distinguished Young Scholars (51925301), the Science Fund for Distinguished Young Scholars of Beijing Natural Science Foundation (JQ180003), Wanren Plan (wrjh201903), and Hebei Province High School Science and Technology Research Project (QN2020223).

Notes and references

1 J. Shintake, V. Cacucciolo, D. Floreano and H. Shea, Soft robotic grippers, *Adv. Mater.*, 2018, **30**, 1707035.
2 Y. Ji, X. Lin, Z. Wu, Y. Wu, W. Gao and Q. He, Macroscale chemotaxis from a swarm of bacteria-mimicking nanoswimmers, *Angew. Chem., Int. Ed.*, 2019, **58**, 12200.
3 Y. Ji, X. Lin, H. Zhang, Y. Wu, J. Li and Q. He, Thermoresponsive polymer brush modulation on the direction of motion of phoretically driven janus micromotors, *Angew. Chem., Int. Ed.*, 2019, **58**, 4184.
4 R. García-Álvarez, L. Chen, A. Nedilko, A. Sánchez-Iglesias, A. Rix, W. Lederle, V. Pathak, T. Lammers, G. von Plessen, K. Kostarelos, L. M. Liz-Marzán, A. J. C. Kuehne and D. N. Chigrin, Optimizing the geometry of photoacoustically active gold nanoparticles for biomedical imaging, *ACS Photonics*, 2020, **7**, 646.
5 T. Repenko, A. Rix, S. Ludwanowski, D. Go, F. Kiessling, W. Lederle and A. J. C. Kuehne, Bio-degradable highly fluorescent conjugated polymer nanoparticles for biomedical imaging applications, *Nat. Commun.*, 2017, **8**, 470.
6 J. Linkhorst, J. Rabe, L. T. Hirschwald, A. J. C. Kuehne and M. Wessling, Direct observation of deformation in microgel filtration, *Sci. Rep.*, 2019, **9**, 18998.
7 Z. Lin, C. Gao, M. Chen, X. Lin and Q. He, Collective motion and dynamic self-assembly of colloid motors, *Curr. Opin. Colloid Interface Sci.*, 2018, **35**, 51.
8 H. Xie, M. Sun, X. Fan, Z. Lin, W. Chen, L. Wang, L. Dong and Q. He, Reconfigurable magnetic microrobot swarm: Multimode transformation, locomotion, and manipulation, *Sci. Robot.*, 2019, **4**, eaav8006.
9 F.-J. Lin, C. Guo, W.-T. Chuang, C.-L. Wang, Q. Wang, H. Liu, C.-S. Hsu and L. Jiang, Directional solution coating by the Chinese brush: A facile approach to improving molecular alignment for high-performance polymer tfts, *Adv. Mater.*, 2017, **29**, 1606987.
10 P. Wang, R. Bian, Q. a. Meng, H. Liu and L. Jiang, Bioinspired dynamic wetting on multiple fibers, *Adv. Mater.*, 2017, **29**, 1703042.
11 M. Hendrikx, J. ter Schiphorst, E. P. A. van Heeswijk, G. Koçer, C. Knie, D. Bléger, S. Hecht, P. Jonkheijm, D. J. Broer and A. P. H. J. Schenning, Re- and preconfigurable multistable visible light responsive surface topographies, *Small*, 2018, **14**, 1803274.
12 G. Koçer, J. ter Schiphorst, M. Hendrikx, H. G. Kassa, P. Leclère, A. P. H. J. Schenning and P. Jonkheijm, Light-responsive hierarchically structured liquid crystal polymer networks for harnessing cell adhesion and migration, *Adv. Mater.*, 2017, **29**, 1606407.

13 C. Ma, W. Lu, X. Yang, J. He, X. Le, L. Wang, J. Zhang, M. J. Serpe, Y. Huang and T. Chen, Bioinspired anisotropic hydrogel actuators with on–off switchable and color-tunable fluorescence behaviors, *Adv. Funct. Mater.*, 2018, **28**, 1704568.
14 Y. Wang, H. Cui, Q. Zhao and X. Du, Chameleon-inspired structural-color actuators, *Matter*, 2019, **1**, 626.
15 T. Mitsumata, K. Ikeda, J. P. Gong and Y. Osada, Solvent-driven chemical motor, *Appl. Phys. Lett.*, 1998, **73**, 2366.
16 Y. Gao, M. Cheng, B. Wang, Z. Feng and F. Shi, Diving–surfacing cycle within a stimulus-responsive smart device towards developing functionally cooperating systems, *Adv. Mater.*, 2010, **22**, 5125.
17 G. Ju, M. Cheng, M. Xiao, J. Xu, K. Pan, X. Wang, Y. Zhang and F. Shi, Smart transportation between three phases through a stimulus-responsive functionally cooperating device, *Adv. Mater.*, 2013, **25**, 2915.
18 S. K. Sailapu and A. Chattopadhyay, Induction of electromotive force by an autonomously moving magnetic bot, *Angew. Chem., Int. Ed.*, 2014, **53**, 1521.
19 M. Song, M. Cheng, G. Ju, Y. Zhang and F. Shi, Converting chemical energy into electricity through a functionally cooperating device with diving–surfacing cycles, *Adv. Mater.*, 2014, **26**, 7059.
20 L. Yu, M. Cheng, M. Song, D. Zhang, M. Xiao and F. Shi, pH-Responsive round-way motions of a smart device through integrating two types of chemical actuators in one smart system, *Adv. Funct. Mater.*, 2015, **25**, 5786.
21 L. Zhang, M. Song, M. Xiao and F. Shi, Diving–surfacing smart locomotion driven by a CO_2-forming reaction, with applications to minigenerators, *Adv. Funct. Mater.*, 2016, **26**, 851.
22 M. Song, M. Cheng, M. Xiao, L. Zhang, G. Ju and F. Shi, Biomimicking of a swim bladder and its application as a mini-generator, *Adv. Mater.*, 2017, **29**, 1603312.
23 X. Yang, M. Cheng, L. Zhang, S. Zhang, X. Liu and F. Shi, Electricity generation through light-responsive diving–surfacing locomotion of a functionally cooperating smart device, *Adv. Mater.*, 2018, **30**, 1803125.
24 M. Frenkel, A. Vilk, I. Legchenkova, S. Shoval and E. Bormashenko, Mini-generator of electrical power exploiting the Marangoni flow inspired self-propulsion, *ACS Omega*, 2019, **4**, 15265.
25 M. Mammen, S.-K. Choi and G. M. Whitesides, Polyvalent interactions in biological systems: Implications for design and use of multivalent ligands and inhibitors, *Angew. Chem., Int. Ed.*, 1998, **37**, 2754.
26 C. A. Hunter and H. L. Anderson, What is cooperativity?, *Angew. Chem., Int. Ed.*, 2009, **48**, 7488.
27 C. Fasting, C. A. Schalley, M. Weber, O. Seitz, S. Hecht, B. Koksch, J. Dernedde, C. Graf, E.-W. Knapp and R. Haag, Multivalency as a chemical organization and action principle, *Angew. Chem., Int. Ed.*, 2012, **51**, 10472.
28 J. Dernedde, in *Multivalency: Concepts, research & applications*, ed. J. Huskens, L. J. Prins, R. Haag and B. J. Ravoo, Wiley-VCH, Weinheim, 2017, ch. 4, vol. 4, p. 103.
29 K. Y. Ma, P. Chirarattananon, S. B. Fuller and R. J. Wood, Controlled flight of a biologically inspired, insect-scale robot, *Science*, 2013, **340**, 603.
30 L. Zhang, Y. Yuan, X. Qiu, T. Zhang, Q. Chen and X. Huang, Marangoni effect-driven motion of miniature robots and generation of electricity on water, *Langmuir*, 2017, **33**, 12609.
31 M. Xiao, M. Cheng, Y. Zhang and F. Shi, Combining the Marangoni effect and the pH-responsive superhydrophobicity–superhydrophilicity transition to biomimic the locomotion process of the beetles of Genus Stenus, *Small*, 2013, **9**, 2509.
32 M. Cheng, G. Ju, Y. Zhang, M. Song, Y. Zhang and F. Shi, Supramolecular assembly of macroscopic building blocks through self-propelled locomotion by dissipating chemical energy, *Small*, 2014, **10**, 3907.
33 M. Xiao, Y. Xian and F. Shi, Precise macroscopic supramolecular assembly by combining spontaneous locomotion driven by the Marangoni effect and molecular recognition, *Angew. Chem., Int. Ed.*, 2015, **54**, 8952.
34 M. Cheng, G. Zhu, L. Li, S. Zhang, D. Zhang, A. J. C. Kuehne and F. Shi, Parallel and precise macroscopic supramolecular assembly through prolonged Marangoni motion, *Angew. Chem., Int. Ed.*, 2018, **57**, 14106.
35 G. Ju, X. Yang, L. Li, M. Cheng and F. Shi, Removal of oil spills through a self-propelled smart device, *Chem. – Asian J.*, 2019, **14**, 2435.
36 L. Zhang, M. Cheng, H. Luo, H. Zhang, G. Ju, P. Liu, Y. Zhou and F. Shi, Mini-generator based on reciprocating vertical motions driven by intracorporeal energy, *Adv. Healthcare Mater.*, 2019, **8**, 1900060.
37 R. Lorenz, Finite-time thermodynamics of an instrumented drinking bird toy, *Am. J. Phys.*, 2006, **74**, 677.
38 S. T. Uechi, H. Uechi and A. Nishimura, The analysis of thermomechanical periodic motions of a drinking bird, *World J. Eng. Technol.*, 2019, **7**, 559.
39 H. Uechi and S. T. Uechi, Thermoelectric energy conversion of a drinking bird by disk-magnet electromagnetic induction, *World J. Eng. Technol.*, 2020, **8**, 204.
40 D. L. Hu, B. Chan and J. W. M. Bush, The hydrodynamics of water strider locomotion, *Nature*, 2003, **424**, 663.
41 F. Shi, J. Niu, J. Liu, F. Liu, Z. Wang, X.-Q. Feng and X. Zhang, Towards understanding why a superhydrophobic coating is needed by water striders, *Adv. Mater.*, 2007, **19**, 2257.
42 M. Cheng, Q. Liu, G. Ju, Y. Zhang, L. Jiang and F. Shi, Bell-shaped superhydrophilic–superhydrophobic–superhydrophilic double transformation on a pH-responsive smart surface, *Adv. Mater.*, 2014, **26**, 306.
43 P. Chen, Y. Xu, S. He, X. Sun, S. Pan, J. Deng, D. Chen and H. Peng, Hierarchically arranged helical fibre actuators driven by solvents and vapours, *Nat. Nanotechnol.*, 2015, **10**, 1077.
44 M. Xiao, L. Wang, F. Ji and F. Shi, Converting chemical energy to electricity through a three-jaw mini-generator driven by the decomposition of hydrogen peroxide, *ACS Appl. Mater. Interfaces*, 2016, **8**, 11403.

45 H. Cheng, Y. Hu, F. Zhao, Z. Dong, Y. Wang, N. Chen, Z. Zhang and L. Qu, Moisture-activated torsional graphene-fiber motor, *Adv. Mater.*, 2014, **26**, 2909.
46 L. S. Y. Wong, S. Hossain, A. Ta, J. Edvinsson, D. H. Rivas and H. Naas, A very low-power CMOS mixed-signal IC for implantable pacemaker applications, *IEEE J. Solid-State Circuits*, 2004, **39**, 2446.
47 Z. L. Wang, J. Chen and L. Lin, Progress in triboelectric nanogenerators as a new energy technology and self-powered sensors, *Energy Environ. Sci.*, 2015, **8**, 2250.
48 G. Zhu, B. Peng, J. Chen, Q. Jing and Z. Lin, Wang, Triboelectric nanogenerators as a new energy technology: From fundamentals, devices, to applications, *Nano Energy*, 2015, **14**, 126.
49 C. Wu, A. C. Wang, W. Ding, H. Guo and Z. L. Wang, Triboelectric nanogenerator: A foundation of the energy for the new era, *Adv. Energy Mater.*, 2019, **9**, 1802906.
50 F.-R. Fan, Z.-Q. Tian and Z. Lin, Wang, Flexible triboelectric generator, *Nano Energy*, 2012, **1**, 328.
51 J. Chen and Z. L. Wang, Reviving vibration energy harvesting and self-powered sensing by a triboelectric nanogenerator, *Joule*, 2017, **1**, 480.
52 Z. L. Wang, On Maxwell's displacement current for energy and sensors: The origin of nanogenerators, *Mater. Today*, 2017, **20**, 74.
53 W. Ding, A. C. Wang, C. Wu, H. Guo and Z. L. Wang, Human–machine interfacing enabled by triboelectric nanogenerators and tribotronics, *Adv. Mater. Technol.*, 2019, **4**, 1800487.
54 A. Chen, C. Zhang, G. Zhu and Z. L. Wang, Polymer materials for high-performance triboelectric nanogenerators, *Adv. Sci.*, 2020, **7**, 2000186.
55 J. Tian, X. Chen and Z. L. Wang, Environmental energy harvesting based on triboelectric nanogenerators, *Nanotechnology*, 2020, **31**, 242001.
56 K. Dong, X. Peng and Z. L. Wang, Fiber/fabric-based piezoelectric and triboelectric nanogenerators for flexible/stretchable and wearable electronics and artificial intelligence, *Adv. Mater.*, 2020, **32**, 1902549.
57 B. Burger, P. M. Maffettone, V. V. Gusev, C. M. Aitchison, Y. Bai, X. Wang, X. Li, B. M. Alston, B. Li, R. Clowes, N. Rankin, B. Harris, R. S. Sprick and A. I. Cooper, A mobile robotic chemist, *Nature*, 2020, **583**, 237.
58 J. Teyssier, S. V. Saenko, D. van der Marel and M. C. Milinkovitch, Photonic crystals cause active colour change in chameleons, *Nat. Commun.*, 2015, **6**, 6368.
59 M. Xiao, M. Cheng and F. Shi, Self-propelling mini-motor and its applications in supramolecular self-assembly and energy conversion, *Sci. Sin.: Chim.*, 2017, **47**, 40.
60 F. Shi, Z. Wang and X. Zhang, Combining a layer-by-layer assembling technique with electrochemical deposition of gold aggregates to mimic the legs of water striders, *Adv. Mater.*, 2005, **17**, 1005.
61 H. Dong, M. Cheng, Y. Zhang, H. Wei and F. Shi, Extraordinary drag-reducing effect of a superhydrophobic coating on a macroscopic model ship at high speed, *J. Mater. Chem. A*, 2013, **1**, 5886.
62 M. Cheng, M. Song, H. Dong and F. Shi, Surface adhesive forces: A metric describing the drag-reducing effects of superhydrophobic coatings, *Small*, 2015, **11**, 1665.
63 M. Cheng, S. Zhang, H. Dong, S. Han, H. Wei and F. Shi, Improving the durability of a drag-reducing nanocoating by enhancing its mechanical stability, *ACS Appl. Mater. Interfaces*, 2015, **7**, 4275.
64 Z. Wang, S. Zhang, S. Gao, X. Ouyang, J. Li, R. Li, H. Wei, Z. Shuai, W. Li and S. Lyu, A simple, low-cost method to fabricate drag-reducing coatings on a macroscopic model ship, *Chem. Res. Chin. Univ.*, 2018, **34**, 616.
65 R. F. Ismagilov, A. Schwartz, N. Bowden and G. M. Whitesides, Autonomous movement and self-assembly, *Angew. Chem., Int. Ed.*, 2002, **41**, 652.
66 M. Xiao, C. Jiang and F. Shi, Design of a UV-responsive microactuator on a smart device for light-induced on-off-on motion, *NPG Asia Mater.*, 2014, **6**, e128.
67 G. Zhao and M. Pumera, Macroscopic self-propelled objects, *Chem. – Asian J.*, 2012, **7**, 1994.
68 D. Okawa, S. J. Pastine, A. Zettl and J. M. J. Fréchet, Surface tension mediated conversion of light to work, *J. Am. Chem. Soc.*, 2009, **131**, 5396.
69 T. Zhao, X. Zhu, L. Zhang, H. Cang, X. Zhang, C. Li, H. Wei and N. Ma, Dual-responsive self-propulsion smart device steadily driven by CO_2 and H_2O_2, *ACS Appl. Mater. Interfaces*, 2018, **10**, 4095.
70 M. Xiao, X. Guo, M. Cheng, G. Ju, Y. Zhang and F. Shi, pH-Responsive on-off motion of a superhydrophobic boat: Towards the design of a minirobot, *Small*, 2014, **10**, 859.
71 X. Li, F. Mou, J. Guo, Z. Deng, C. Chen, L. Xu, M. Luo and J. Guan, Hydrophobic janus foam motors: Self-propulsion and on-the-fly oil absorption, *Micromachines*, 2018, **9**, 23.
72 X. Zhang, Q. Zhang, L. Zhang, P. Li, M. Cheng, J. Zhao, Y. Zhang, H. Su, T. Tan and F. Shi, Functionally cooperating mini-generator: From bacterial fermentation to electricity, *Adv. Funct. Mater.*, 2019, **29**, 1900879.
73 S. Nakata, Y. Iguchi, S. Ose, M. Kuboyama, T. Ishii and K. Yoshikawa, Self-rotation of a camphor scraping on water: New insight into the old problem, *Langmuir*, 1997, **13**, 4454.
74 Y. Matsuda, N. J. Suematsu, H. Kitahata, Y. S. Ikura and S. Nakata, Acceleration or deceleration of self-motion by the Marangoni effect, *Chem. Phys. Lett.*, 2016, **654**, 92.
75 M. Cheng, D. Zhang, S. Zhang, Z. Wang and F. Shi, Tackling the short-lived Marangoni motion using a supramolecular strategy, *CCS Chem.*, 2019, **1**, 148.
76 T. Mitsumata, K. Ikeda, J. P. Gong and Y. Osada, Controlled motion of solvent-driven gel motor and its application as a generator, *Langmuir*, 2000, **16**, 307.
77 Y. Ikezoe, G. Washino, T. Uemura, S. Kitagawa and H. Matsui, Autonomous motors of a metal–organic framework powered by reorganization of self-assembled peptides at interfaces, *Nat. Mater.*, 2012, **11**, 1081.
78 Y. Ikezoe, J. Fang, T. L. Wasik, T. Uemura, Y. Zheng, S. Kitagawa and H. Matsui, Peptide assembly-driven metal–organic framework (MOF) motors for micro electric generators, *Adv. Mater.*, 2015, **27**, 288.

79 Y. S. Ikura, R. Tenno, H. Kitahata, N. J. Suematsu and S. Nakata, Suppression and regeneration of camphor-driven Marangoni flow with the addition of sodium dodecyl sulfate, *J. Phys. Chem. B*, 2012, **116**, 992.
80 S. Nakata, K. Nasu, Y. Irie and S. Hatano, Self-propelled motion of a camphor disk on a photosensitive amphiphilic molecular layer, *Langmuir*, 2019, **35**, 4233.
81 S. Nakata and R. Fujita, Self-propelled motion of a camphor disk on a nervonic acid molecular layer and its dependence on phase transition, *J. Phys. Chem. B*, 2020, **124**, 5525.
82 H. Jin, A. Marmur, O. Ikkala and R. H. A. Ras, Vapour-driven Marangoni propulsion: Continuous, prolonged and tunable motion, *Chem. Sci.*, 2012, **3**, 2526.
83 A. Musin, R. Grynyov, M. Frenkel and E. Bormashenko, Self-propulsion of a metallic superoleophobic micro-boat, *J. Colloid Interface Sci.*, 2016, **479**, 182.
84 R. Sharma, S. T. Chang and O. D. Velev, Gel-based self-propelling particles get programmed to dance, *Langmuir*, 2012, **28**, 10128.
85 K. Furukawa, T. Teshima and Y. Ueno, Self-propelled ion gel at air-water interface, *Sci. Rep.*, 2017, **7**, 9323.
86 M. Song, M. Xiao, L. Zhang, D. Zhang, Y. Liu, F. Wang and F. Shi, Generating induced current through the diving-surfacing motion of a stimulus–responsive smart device, *Nano Energy*, 2016, **20**, 233.
87 S. H. Kim, C. S. Haines, N. Li, K. J. Kim, T. J. Mun, C. Choi, J. Di, Y. J. Oh, J. P. Oviedo, J. Bykova, S. Fang, N. Jiang, Z. Liu, R. Wang, P. Kumar, R. Qiao, S. Priya, K. Cho, M. Kim, M. S. Lucas, L. F. Drummy, B. Maruyama, D. Y. Lee, X. Lepró, E. Gao, D. Albarq, R. Ovalle-Robles, S. J. Kim and R. H. Baughman, Harvesting electrical energy from carbon nanotube yarn twist, *Science*, 2017, **357**, 773.
88 Z.-L. Zhao, S. Zhou, S. Xu, X.-Q. Feng and Y. M. Xie, High-speed spinning disks on flexible threads, *Sci. Rep.*, 2017, **7**, 13111.
89 S. H. Kim, H. J. Sim, J. S. Hyeon, D. Suh, G. M. Spinks, R. H. Baughman and S. J. Kim, Harvesting electrical energy from torsional thermal actuation driven by natural convection, *Sci. Rep.*, 2018, **8**, 8712.
90 S. M. Mirvakili and I. W. Hunter, Artificial muscles: Mechanisms, applications, and challenges, *Adv. Mater.*, 2018, **30**, 1704407.
91 D. Zhang, J. Liu, B. Chen, J. Wang and L. Jiang, Research progress of solvent-based smart actuator materials, *Acta Chim. Sin.*, 2018, **76**, 425.
92 B. Fang, Y. Xiao, Z. Xu, D. Chang, B. Wang, W. Gao and C. Gao, Handedness-controlled and solvent-driven actuators with twisted fibers, *Mater. Horiz.*, 2019, **6**, 1207.
93 X. Chen, L. Mahadevan, A. Driks and O. Sahin, Bacillus spores as building blocks for stimuli-responsive materials and nanogenerators, *Nat. Nanotechnol.*, 2014, **9**, 137.
94 X. Chen, D. Goodnight, Z. Gao, A. H. Cavusoglu, N. Sabharwal, M. DeLay, A. Driks and O. Sahin, Scaling up nanoscale water-driven energy conversion into evaporation-driven engines and generators, *Nat. Commun.*, 2015, **6**, 7346.
95 R. Tang, Z. Liu, D. Xu, J. Liu, L. Yu and H. Yu, Optical pendulum generator based on photomechanical liquid-crystalline actuators, *ACS Appl. Mater. Interfaces*, 2015, **7**, 8393.
96 R. Lan, J. Sun, C. Shen, R. Huang, Z. Zhang, L. Zhang, L. Wang and H. Yang, Near-infrared photodriven self-sustained oscillation of liquid-crystalline network film with predesignated polydopamine coating, *Adv. Mater.*, 2020, **32**, 1906319.
97 J. Gong, H. Lin, J. W. C. Dunlop and J. Yuan, Hierarchically arranged helical fiber actuators derived from commercial cloth, *Adv. Mater.*, 2017, **29**, 1605103.
98 W. Wang, C. Xiang, Q. Liu, M. Li, W. Zhong, K. Yan and D. Wang, Natural alginate fiber-based actuator driven by water or moisture for energy harvesting and smart controller applications, *J. Mater. Chem. A*, 2018, **6**, 22599.
99 S. H. Kim, M. D. Lima, M. E. Kozlov, C. S. Haines, G. M. Spinks, S. Aziz, C. Choi, H. J. Sim, X. Wang, H. Lu, D. Qian, J. D. W. Madden, R. H. Baughman and S. J. Kim, Harvesting temperature fluctuations as electrical energy using torsional and tensile polymer muscles, *Energy Environ. Sci.*, 2015, **8**, 3336.
100 Y. Hu, J. Yang, S. Niu, W. Wu and Z. L. Wang, Hybridizing triboelectrification and electromagnetic induction effects for high-efficient mechanical energy harvesting, *ACS Nano*, 2014, **8**, 7442.
101 T. Quan, X. Wang, Z. L. Wang and Y. Yang, Hybridized electromagnetic–triboelectric nanogenerator for a self-powered electronic watch, *ACS Nano*, 2015, **9**, 12301.
102 K. Zhang, X. Wang, Y. Yang and Z. L. Wang, Hybridized electromagnetic–triboelectric nanogenerator for scavenging biomechanical energy for sustainably powering wearable electronics, *ACS Nano*, 2015, **9**, 3521.
103 X. Wang, S. Wang, Y. Yang and Z. L. Wang, Hybridized electromagnetic–triboelectric nanogenerator for scavenging air-flow energy to sustainably power temperature sensors, *ACS Nano*, 2015, **9**, 4553.
104 B. Zhang, J. Chen, L. Jin, W. Deng, L. Zhang, H. Zhang, M. Zhu, W. Yang and Z. L. Wang, Rotating-disk-based hybridized electromagnetic–triboelectric nanogenerator for sustainably powering wireless traffic volume sensors, *ACS Nano*, 2016, **10**, 6241.
105 P. Wang, L. Pan, J. Wang, M. Xu, G. Dai, H. Zou, K. Dong and Z. L. Wang, An ultra-low-friction triboelectric–electromagnetic hybrid nanogenerator for rotation energy harvesting and self-powered wind speed sensor, *ACS Nano*, 2018, **12**, 9433.
106 Z. Wen, H. Guo, Y. Zi, M.-H. Yeh, X. Wang, J. Deng, J. Wang, S. Li, C. Hu, L. Zhu and Z. L. Wang, Harvesting broad frequency band blue energy by a triboelectric–electromagnetic hybrid nanogenerator, *ACS Nano*, 2016, **10**, 6526.
107 Z. Wu, H. Guo, W. Ding, Y.-C. Wang, L. Zhang and Z. L. Wang, A hybridized triboelectric–electromagnetic water wave energy harvester based on a magnetic sphere, *ACS Nano*, 2019, **13**, 2349.

108 G. M. Whitesides and B. Grzybowski, Self-assembly at all scales, *Science*, 2002, **295**, 2418.
109 A. Harada, R. Kobayashi, Y. Takashima, A. Hashidzume and H. Yamaguchi, Macroscopic self-assembly through molecular recognition, *Nat. Chem.*, 2011, **3**, 34.
110 M. Cheng, H. Gao, Y. Zhang, W. Tremel, J.-F. Chen, F. Shi and W. Knoll, Combining magnetic field induced locomotion and supramolecular interaction to micromanipulate glass fibers: Toward assembly of complex structures at mesoscale, *Langmuir*, 2011, **27**, 6559.
111 M. Cheng, Q. Zhang and F. Shi, Macroscopic supramolecular assembly: New concept for the fabrication of supramolecular materials, *Sci. Sin.: Chim.*, 2017, **47**, 816.
112 M.-J. Cheng, Q. Zhang and F. Shi, Macroscopic supramolecular assembly and its applications, *Chin. J. Polym. Sci.*, 2018, **36**, 306.
113 M. Cheng and F. Shi, Precise macroscopic supramolecular assembly: Strategies and applications, *Chem. – Eur. J.*, 2020, DOI: 10.1002/chem.202001881.
114 M. Cheng and F. Shi, Precise macroscopic supramolecular assembly, *Acta Polym. Sin.*, 2020, **51**, 598.
115 T. V. Vinay, T. N. Banuprasad, S. D. George, S. Varghese and S. N. Varanakkottu, Additive-free tunable transport and assembly of floating objects at water-air interface using bubble-mediated capillary forces, *Adv. Mater. Interfaces*, 2017, **4**, 1601231.
116 M. Cheng, F. Shi, J. Li, Z. Lin, C. Jiang, M. Xiao, L. Zhang, W. Yang and T. Nishi, Macroscopic supramolecular assembly of rigid building blocks through a flexible spacing coating, *Adv. Mater.*, 2014, **26**, 3009.
117 R. Akram, M. Cheng, F. Guo, S. Iqbal and F. Shi, Toward understanding whether interactive surface area could direct ordered macroscopic supramolecular self-assembly, *Langmuir*, 2016, **32**, 3617.
118 Q. Zhang, C. Liu, G. Ju, M. Cheng and F. Shi, Macroscopic supramolecular assembly through electrostatic interactions based on a flexible spacing coating, *Macromol. Rapid Commun.*, 2018, **39**, 1800180.
119 G. Ju, Q. Zhang, F. Guo, P. Xie, M. Cheng and F. Shi, Macroscopic supramolecular assembly of rigid hydrogels assisted by a flexible spacing coating, *J. Mater. Chem. B*, 2019, **7**, 1684.
120 Y. Duan, Q. An, Q. Zhang and Y. Zhang, Smoothing of fast assembled layer-by-layer films by adjusting assembly conditions, *Chem. Res. Chin. Univ.*, 2015, **31**, 674.
121 C. Liu, Q. Zhang, Y. Zhang, M. Cheng and F. Shi, Macroscopic supramolecular assembly through adjusting the surface-flexibility of the building block, *Chin. Sci. Bull.*, 2018, **63**, 3650.
122 Q. Xia, S. Pan, Y. Zhang, Q. An, Q. Zhang and Y. Zhang, Preparation of highly loaded paa/pah layer-by-layer films by combining acid transformation and templating methods, *Chem. Res. Chin. Univ.*, 2019, **35**, 353.

